

ROBUST APPROXIMATION OF GENERALIZED BIOT-BRINKMAN PROBLEMS

QINGGUO HONG^{*}, JOHANNES KRAUS[†], MIROSLAV KUČHTA[‡], MARIA LYMBERY[§],
KENT-ANDRÉ MARDAL[¶], AND MARIE E. ROGNES^{||}

Abstract. The generalized Biot-Brinkman equations describe the displacement, pressures and fluxes in an elastic medium permeated by multiple viscous fluid networks and can be used to study complex poromechanical interactions in geophysics, biophysics and other engineering sciences. These equations extend on the Biot and multiple-network poroelasticity equations on the one hand and Brinkman flow models on the other hand, and as such embody a range of singular perturbation problems in realistic parameter regimes. In this paper, we introduce, theoretically analyze and numerically investigate a class of three-field finite element formulations of the generalized Biot-Brinkman equations. By introducing appropriate norms, we demonstrate that the proposed finite element discretization, as well as an associated preconditioning strategy, is robust with respect to the relevant parameter regimes. The theoretical analysis is complemented by numerical examples.

Key words. poromechanics, finite element method, preconditioning, Biot equations, Brinkman approximation, multiple-network poroelasticity

1. Introduction. The study of the mechanical response of fluid-filled porous media – *poromechanics* – is essential in geophysics, biophysics and civil engineering. Through a series of seminal works dating from 1941 and onwards [7, 8], Biot introduced governing equations for the dynamic behavior of a linearly elastic solid matrix permeated by a viscous fluid with flow through the pore network described by Darcy’s law [17, 47]. Double-porosity models, extending upon Biot’s single fluid network to the case of two interacting networks, were used to describe the motion of liquids in fissured rocks as early as in the 1960s [5, 48, 32]. Later, multiple-network poroelasticity equations emerged in the context of reservoir modelling [4] to describe elastic media permeated by multiple networks characterised by different porosities, permeabilities and/or interactions. Since the early 2000s, poromechanics has been applied to model the heart [38, 13] as well as the brain and central nervous system [45, 44, 46, 16, 20].

In addition to interactions between fluid networks, recently also the viscous forces acting within each network have come to the fore [6, 14, 12, 31]. At its core, the effect of viscosity can be accounted for by replacing the Darcy approximation in the poroelasticity model by a Brinkman approximation [11, 40]. We here introduce multiple-network poroelasticity models incorporating viscosity under the term *generalized Biot-Brinkman equations*. In a bounded domain $\Omega \subset \mathbb{R}^d$, $d = 1, 2, 3$ comprising n fluid networks, the generalized Biot-Brinkman equations read as follows: find the displacement $\mathbf{u} = \mathbf{u}(x, t)$, fluid fluxes $\mathbf{v}_i = \mathbf{v}_i(x, t)$ and corresponding (negative) fluid

^{*}Department of Mathematics, Pennsylvania State University (huq11@psu.edu).

[†]Faculty of Mathematics, University of Duisburg-Essen (johannes.kraus@uni-due.de).

[‡]Department of Numerical Analysis and Scientific Computing, Simula Research Laboratory (miroslav@simula.no).

[§]Faculty of Mathematics, University of Duisburg-Essen (maria.lymbery@uni-due.de).

[¶]Department of Mathematics, University of Oslo and Department for Numerical Analysis and Scientific Computing, Simula Research Laboratory (kent-and@simula.no).

^{||}Department of Numerical Analysis and Scientific Computing, Simula Research Laboratory and Department of Mathematics, University of Bergen (meg@simula.no).

pressures $p_i = p_i(x, t)$, for $i = 1, \dots, n$ satisfying

$$(1.1a) \quad -\operatorname{div}(\boldsymbol{\sigma}(\mathbf{u}) + \boldsymbol{\alpha} \cdot \mathbf{p}\mathbf{I}) = \mathbf{f},$$

$$(1.1b) \quad -\nu_i \operatorname{div} \boldsymbol{\varepsilon}(\mathbf{v}_i) + \mathbf{v}_i - K_i \nabla p_i = \mathbf{r}_i,$$

$$(1.1c) \quad -c_i \dot{p}_i - \bar{\beta}_i p_i + \alpha_i \operatorname{div} \dot{\mathbf{u}} + \operatorname{div} \mathbf{v}_i + \boldsymbol{\beta}_i \cdot \mathbf{p} = g_i,$$

over $\Omega \times (0, T)$ for $T > 0$, and where (1.1b) and (1.1c) hold for $i = 1, \dots, n$. In (1.1a), we have introduced the vector notation $\mathbf{p} = (p_1, \dots, p_n)$ and $\boldsymbol{\alpha} = (\alpha_1, \dots, \alpha_n)$, where α_i is the Biot-Willis coefficient associated with network i . The elastic stress and strain tensors are:

$$(1.2) \quad \boldsymbol{\sigma}(\mathbf{u}) = 2\mu \boldsymbol{\varepsilon}(\mathbf{u}) + \lambda \operatorname{div}(\mathbf{u})\mathbf{I}, \quad \boldsymbol{\varepsilon}(\mathbf{u}) = \frac{1}{2}(\nabla \mathbf{u} + (\nabla \mathbf{u})^T),$$

respectively, and with Lamé parameters μ and λ . Moreover, for each fluid network i , ν_i denotes the fluid viscosity and K_i is its hydraulic conductance tensor. Furthermore, (1.1c) is an equivalent formulation of the standard multiple-network poroelasticity mass balance equations [4, 36, 24] with transfer coefficients β_{ij} , denoting $\boldsymbol{\beta}_i = (\beta_{i1}, \dots, \beta_{in})$ and $\bar{\beta}_i = \sum_j \beta_{ij}$, when the fluid transfer into network i is given by

$$\sum_{j=1, j \neq i}^n \beta_{ij}(p_i - p_j).$$

The constants c_i in (1.1c) denote the constrained specific storage coefficients, see e.g. [43] and the references therein. Finally, the prescribed right hand side \mathbf{f} denotes body forces, while g_i denotes a fluid source and \mathbf{r}_i represents an external flux, both of the two latter in each network i . In the case $n = 1$ and $\nu = 0$, (1.1) reduces to the Biot equations.

The generalized Biot-Brinkman problem (1.1) defines a challenging system of PDEs to solve numerically. One reason for this is the large number of material parameters, several of which give rise to singular perturbation problems such as in the extreme cases of (near) incompressibility ($\lambda \rightarrow \infty$) and impermeability ($K_i \rightarrow 0$). Specifically, $\lambda \gg \mu$ is associated with numerical locking; if (1.1) is scaled by $1/\lambda$, the elastic term of the equation reads $\operatorname{div} \frac{2\mu}{\lambda} \boldsymbol{\varepsilon}(\mathbf{u}) + \nabla \operatorname{div} \mathbf{u} = \mathbf{f}$ which transforms from an H^1 problem to an $H(\operatorname{div})$ problem as λ tends to infinity. Similar singular perturbation problems arise, now for the flux variable \mathbf{v}_i , as ν_i tends to zero. Furthermore, certain parameter ranges of the storage coefficients and permeabilities ($K_i \ll c_i$) give rise to singular perturbation problems in the Darcy sub-system, see e.g. [37] and references therein. Finally, we mention that large transfer coefficients β_{ij} and/or small Biot-Willis coefficients α_i can lead to strong coupling of the different subsystems and prevent direct exploitation of each subsystem's properties.

In the case of vanishing viscosities ($\nu_i = 0, \forall i$) the system (1.1) reduces to the multiple-network poroelasticity (MPET) equations. Robust and conservative numerical approximations of the MPET equations have been studied in the context of (near) incompressibility [36] as well as other material parameters [24, 27, 26]. Parameter-independent preconditioning and splitting schemes as well as a-posteriori error analysis and adaptivity have also been identified for the MPET equations [25, 27, 39, 18]. However, the generalized Biot-Brinkman system has received little attention from the numerical community. Therefore, the purpose of this paper is to identify and analyze stable finite element approximation schemes and preconditioning techniques for the time-discrete generalized Biot-Brinkman systems, with particular focus on parameter robustness.

This paper is organized as follows. After introducing notation, context and preliminaries in [Section 2](#), we prove that the time-discrete generalized Biot-Brinkman system is well-posed in appropriate function spaces in [Section 3](#). We introduce a fully discrete generalized Biot-Brinkman problem in [Section 4](#) and prove that the discrete approximations satisfy a near optimal a-priori error estimate in appropriate norms independently of material parameters. We also propose a natural preconditioner. The theoretical analysis is complemented by numerical experiments in [Section 5](#).

2. Preliminaries and notation. In this section of preliminaries, we give assumptions on the material parameters, present a rescaling of a time-discrete generalized Biot-Brinkman system and introduce parameter-weighted norms and function spaces.

2.1. Material parameters. We assume that the elastic Lamé coefficients satisfy the standard conditions $\mu > 0$ and $d\lambda + 2\mu > 0$. The transfer coefficients are such that $\beta_{ij} = \beta_{ji} \geq 0$ for $i \neq j$ while $\beta_{ii} = 0$, and the specific storage coefficients $c_i \geq 0$ for $i = 1, \dots, n$. The Biot-Willis coefficients are bounded between zero and one by construction: $0 < \alpha_i \leq 1$. We also assume that the hydraulic conductances $K_i > 0$ for $i = 1, \dots, n$. Further, our focus will be on the case $\nu_i > 0$. For spatially-varying material parameters, we assume that each of the above conditions holds point-wise and that each parameter field is uniformly bounded from above and below.

2.2. Time discretization, rescaling and structure. Taking an implicit Euler time-discretization of [\(1.1\)](#) with uniform timestep τ , multiplying [\(1.1c\)](#) by τ , rearranging terms and removing the time-dependence from the notation, we obtain the following problem structure to be solved over Ω at each time step: find the unknown displacement $\mathbf{u} = \mathbf{u}(x)$, fluid fluxes $\mathbf{v}_i = \mathbf{v}_i(x)$ and corresponding (negative) fluid pressures $p_i = p_i(x)$, for $i = 1, \dots, n$ satisfying

$$\begin{aligned} -\operatorname{div}(\boldsymbol{\sigma}(\mathbf{u}) + \boldsymbol{\alpha} \cdot \mathbf{p}\mathbf{I}) &= \mathbf{f}, \\ -\nu_i \operatorname{div} \boldsymbol{\varepsilon}(\mathbf{v}_i) + \mathbf{v}_i - K_i \nabla p_i &= \mathbf{r}_i, \\ -(c_i + \tau \bar{\beta}_i) p_i + \alpha_i \operatorname{div} \mathbf{u} + \tau \operatorname{div} \mathbf{v}_i + \tau \boldsymbol{\beta}_i \cdot \mathbf{p} &= \tau g_i. \end{aligned}$$

Multiplying by τK_i^{-1} in the second equation(s) for the sake of symmetry gives

$$\begin{aligned} (2.2a) \quad & -\operatorname{div}(\boldsymbol{\sigma}(\mathbf{u}) + \boldsymbol{\alpha} \cdot \mathbf{p}\mathbf{I}) = \mathbf{f}, \\ (2.2b) \quad & -\nu_i \tau K_i^{-1} \operatorname{div} \boldsymbol{\varepsilon}(\mathbf{v}_i) + \tau K_i^{-1} \mathbf{v}_i - \tau \nabla p_i = \tau K_i^{-1} \mathbf{r}_i, \\ (2.2c) \quad & -(c_i + \tau \bar{\beta}_i) p_i + \alpha_i \operatorname{div} \mathbf{u} + \tau \operatorname{div} \mathbf{v}_i + \tau \boldsymbol{\beta}_i \cdot \mathbf{p} = \tau g_i. \end{aligned}$$

For the sake of readability, we define

$$(2.3) \quad s_i := c_i + \tau \bar{\beta}_i, \quad \gamma_i := \tau \nu_i K_i^{-1}$$

recalling that $\bar{\beta}_i = \sum_j \beta_{ij}$ and $\beta_{ii} = 0$, and set

$$(2.4) \quad R^{-1} := \max\{(1 + \nu_1)\tau K_1^{-1}, \dots, (1 + \nu_n)\tau K_n^{-1}\}.$$

Using this notation, we introduce four $n \times n$ parameter matrices

$$(2.5) \quad \Lambda_1 = -\tau \begin{pmatrix} 0 & \beta_{12} & \dots & \beta_{1n} \\ \beta_{21} & 0 & \dots & \beta_{2n} \\ \vdots & \vdots & \ddots & \vdots \\ \beta_{n1} & \beta_{n2} & \dots & 0 \end{pmatrix}$$

and

$$(2.6) \quad \Lambda_2 = \text{diag}(s_1, s_2, \dots, s_n), \quad \Lambda_3 = \tau^2 R I, \quad \Lambda_4 = \frac{1}{2\mu + \lambda} \boldsymbol{\alpha} \boldsymbol{\alpha}^T,$$

before defining

$$(2.7) \quad \Lambda = \sum_{i=1}^4 \Lambda_i.$$

In the case $n = 1$, dropping the subscripts i, j for readability and with the newly introduced parameter notation, the operator structure of the rescaled system (2.2) is

$$(2.8) \quad \begin{pmatrix} -\text{div } \boldsymbol{\sigma} & \mathbf{0} & -\alpha \nabla \\ \mathbf{0} & -\gamma \text{div } \boldsymbol{\varepsilon} + \tau K^{-1} \mathbf{I} & -\tau \nabla \\ \alpha \text{div} & \tau \text{div} & -(\Lambda_1 + \Lambda_2) \end{pmatrix} \begin{pmatrix} \mathbf{u} \\ \mathbf{v} \\ \mathbf{p} \end{pmatrix} = \begin{pmatrix} \mathbf{f} \\ \mathbf{r} \\ \mathbf{g} \end{pmatrix}$$

for $-(\Lambda_1 + \Lambda_2) = c \mathbf{I}$, and $\mathbf{p} = p$ in the $n = 1$ case. The same structure holds for $n > 2$ when denoting $\mathbf{v}^T = (\mathbf{v}_1^T, \mathbf{v}_2^T, \dots, \mathbf{v}_n^T)$, $(\text{Div } \mathbf{v})^T = (\text{div } \mathbf{v}_1, \dots, \text{div } \mathbf{v}_n)$.

By the assumption of symmetric transfer, i.e. $\beta_{ij} = \beta_{ji}$, Λ_1 and Λ are symmetric. Moreover, as $\Lambda_1 + \Lambda_2$ is weakly diagonally dominant and thus symmetric positive semi-definite, Λ_3 is symmetric positive definite, and Λ_4 is symmetric positive semi-definite, it follows that Λ is symmetric positive definite.

2.3. Domain and boundary conditions. Assume that Ω is open and bounded in \mathbb{R}^d , $d = 2, 3$ with Lipschitz boundary $\partial\Omega$. We consider the following idealized boundary conditions for the theoretical analysis of the time-discrete generalized Biot-Brinkman system (2.8) over Ω . We assume that the displacement is prescribed (and equal to zero for simplicity) on the entire boundary $\partial\Omega$. Furthermore for each of the flux momentum equations we assume datum on the normal flux $\mathbf{v}_i \cdot \mathbf{n}$ and the tangential part of the traction associated with the viscous term $\boldsymbol{\varepsilon}(\mathbf{v}_i) \cdot \mathbf{n}$. Combined, we thus set

$$(2.9) \quad \begin{aligned} \mathbf{u}(\mathbf{x}) &= \mathbf{0} & \mathbf{x} \in \partial\Omega, \\ \mathbf{v}_i \cdot \mathbf{n}(\mathbf{x}) &= \mathbf{0}, \quad \mathbf{n} \times (\boldsymbol{\varepsilon}(\mathbf{v}_i) \cdot \mathbf{n})(\mathbf{x}) = \mathbf{0} & \mathbf{x} \in \partial\Omega, \end{aligned}$$

for $i = 1, \dots, n$.

2.4. Function spaces and norms. We use standard notation for the Sobolev spaces $L^2(\Omega)$, $H^1(\Omega)$ and $H(\text{div}, \Omega)$, and denote the $L^2(\Omega)$ -inner product and norm by (\cdot, \cdot) and $\|\cdot\|$, respectively. We let $L_0^2(\Omega)$ denote the space of L^2 functions with zero mean. For a Banach space U , its dual space is denoted U' and the duality pairing between U and U' by $\langle \cdot, \cdot \rangle_{U' \times U}$.

For the displacement, flux and pressure spaces, we define

$$(2.10a) \quad U = \{\mathbf{u} \in H^1(\Omega)^d : \mathbf{u} = \mathbf{0} \text{ on } \partial\Omega\},$$

$$(2.10b) \quad V_i = \{\mathbf{v}_i \in H^1(\Omega)^d : \mathbf{v}_i \cdot \mathbf{n} = 0 \text{ on } \partial\Omega\},$$

$$(2.10c) \quad P_i = L_0^2(\Omega),$$

for $i = 1, \dots, n$, and subsequently define

$$(2.11) \quad V = V_1 \times \dots \times V_n, \quad P = P_1 \times \dots \times P_n.$$

We also equip these spaces with the following parameter-weighted inner products

$$(2.12a) \quad (\mathbf{u}, \mathbf{w})_{\mathbf{U}} = (2\mu\varepsilon(\mathbf{u}), \varepsilon(\mathbf{w})) + \lambda(\operatorname{div} \mathbf{u}, \operatorname{div} \mathbf{w}),$$

$$(2.12b) \quad (\mathbf{v}, \mathbf{z})_{\mathbf{V}} = \sum_{i=1}^n (\gamma_i \varepsilon(\mathbf{v}_i), \varepsilon(\mathbf{z}_i)) + (\tau K_i^{-1} \mathbf{v}_i, \mathbf{z}_i) + (\Lambda^{-1} \tau^2 \operatorname{Div} \mathbf{v}, \operatorname{Div} \mathbf{z}),$$

$$(2.12c) \quad (\mathbf{p}, \mathbf{q})_{\mathbf{P}} = (\Lambda \mathbf{p}, \mathbf{q})$$

and denote the induced norms by $\|\cdot\|_{\mathbf{U}}$, $\|\cdot\|_{\mathbf{V}}$, and $\|\cdot\|_{\mathbf{P}}$, respectively. These are indeed inner products and norms by the assumptions on the material parameters given and in particular the symmetric positive-definiteness of Λ .

3. Well-posedness of the Biot-Brinkman system.

3.1. Abstract form and related results. System (2.8) is a special case of the abstract saddle-point problem

$$(3.1) \quad \begin{pmatrix} A_1 & 0 & B_1^T \\ 0 & A_2 & B_2^T \\ B_1 & B_2 & -A_3 \end{pmatrix} \begin{pmatrix} \mathbf{u} \\ \mathbf{v} \\ \mathbf{p} \end{pmatrix},$$

where $A_1 : \mathbf{U} \rightarrow \mathbf{U}'$, $A_2 : \mathbf{V} \rightarrow \mathbf{V}'$, and $A_3 : \mathbf{P} \rightarrow \mathbf{P}'$ are symmetric and positive (semi-)definite, and $B_1 : \mathbf{U} \rightarrow \mathbf{P}'$, $B_2 : \mathbf{V} \rightarrow \mathbf{P}'$ are linear operators. In terms of bilinear forms, we can write (3.1) as

$$(3.2a) \quad a_1(\mathbf{u}, \mathbf{w}) + b_1(\mathbf{w}, \mathbf{p}) = (\mathbf{f}, \mathbf{w}),$$

$$(3.2b) \quad a_2(\mathbf{v}, \mathbf{z}) + b_2(\mathbf{z}, \mathbf{p}) = (\mathbf{r}, \mathbf{z}),$$

$$(3.2c) \quad b_1(\mathbf{u}, \mathbf{q}) + b_2(\mathbf{v}, \mathbf{q}) - a_3(\mathbf{p}, \mathbf{q}) = (\mathbf{g}, \mathbf{q}).$$

This abstract form was studied in the context of twofold saddle point problems and equivalence of inf-sup stability conditions by Howell and Walkington [30] for the case where $A_3 = A_2 = 0$.

3.2. Three-field variational formulation of the Biot-Brinkman system.

We consider the following variational formulation of the Biot-Brinkman system (2.8) with the boundary conditions given by (2.9): given $\mathbf{f}, \mathbf{r}, \mathbf{g}$, find $(\mathbf{u}, \mathbf{v}, \mathbf{p}) \in \mathbf{U} \times \mathbf{V} \times \mathbf{P}$ such that (3.2) holds with

$$(3.3a) \quad a_1(\mathbf{u}, \mathbf{w}) = (\sigma(\mathbf{u}), \varepsilon(\mathbf{w})),$$

$$(3.3b) \quad a_2(\mathbf{v}, \mathbf{z}) = \sum_{i=1}^n (\gamma_i \varepsilon(\mathbf{v}_i), \varepsilon(\mathbf{z}_i)) + (\tau K_i^{-1} \mathbf{v}_i, \mathbf{z}_i)$$

$$(3.3c) \quad a_3(\mathbf{p}, \mathbf{q}) = \sum_{i=1}^n (s_i p_i, q_i) - \sum_{i,j=1}^n (\tau \beta_{ij} p_j, q_i)$$

$$(3.3d) \quad b_1(\mathbf{w}, \mathbf{p}) = \sum_{i=1}^n (\operatorname{div} \mathbf{w}, \alpha_i p_i) \equiv (\operatorname{div} \mathbf{w}, \boldsymbol{\alpha} \cdot \mathbf{p}),$$

$$(3.3e) \quad b_2(\mathbf{v}, \mathbf{q}) = \sum_{i=1}^n (\tau \operatorname{div} \mathbf{v}_i, q_i),$$

for all $\mathbf{w} \in \mathbf{U}$, $\mathbf{z} \in \mathbf{V}$, and $\mathbf{q} \in \mathbf{P}$. Equivalently, $(\mathbf{u}, \mathbf{v}, \mathbf{p}) \in \mathbf{U} \times \mathbf{V} \times \mathbf{P}$ solves

$$(3.4) \quad \mathcal{A}((\mathbf{u}, \mathbf{v}, \mathbf{p}), (\mathbf{w}, \mathbf{z}, \mathbf{q})) = ((\mathbf{f}, \mathbf{r}, \mathbf{g}), (\mathbf{z}, \mathbf{w}, \mathbf{q}))$$

for all $(\mathbf{z}, \mathbf{w}, \mathbf{q}) \in \mathbf{U} \times \mathbf{V} \times \mathbf{P}$ where

$$(3.5) \quad \begin{aligned} \mathcal{A}((\mathbf{u}, \mathbf{v}, \mathbf{p}), (\mathbf{w}, \mathbf{z}, \mathbf{q})) &= a_1(\mathbf{u}, \mathbf{w}) + a_2(\mathbf{v}, \mathbf{z}) + b_1(\mathbf{w}, \mathbf{p}) + b_1(\mathbf{u}, \mathbf{q}) \\ &\quad + b_2(\mathbf{z}, \mathbf{p}) + b_2(\mathbf{w}, \mathbf{q}) - a_3(\mathbf{p}, \mathbf{q}). \end{aligned}$$

We refer to (3.2)–(3.3), or also (3.4), as a three-field formulation of the Biot-Brinkman system, with three-field referring to the three groups of fields (displacement, fluxes and pressures).

3.3. Stability properties. In this section we prove the main theoretical result of this paper, that is, the uniform well-posedness of problem (3.2)–(3.3) under the norms induced by (2.12), as stated in Theorem 3.5. The proof utilizes the abstract framework for the stability analysis of perturbed saddle-point problems that has recently been presented in [26]. It is performed in two steps. In the first step, we recast the system (3.2)–(3.3) into the following two-by-two (single) perturbed saddle-point problem

$$(3.6) \quad \begin{aligned} \mathcal{A}((\mathbf{u}, \mathbf{v}, \mathbf{p}), (\mathbf{w}, \mathbf{z}, \mathbf{q})) &= \mathcal{A}((\bar{\mathbf{u}}, \mathbf{p}), (\bar{\mathbf{w}}, \mathbf{q})) \\ &= a(\bar{\mathbf{u}}, \bar{\mathbf{w}}) + b(\bar{\mathbf{w}}, \mathbf{p}) + b(\bar{\mathbf{u}}, \mathbf{q}) - c(\mathbf{p}, \mathbf{q}), \end{aligned}$$

where $\bar{\mathbf{u}} = (\mathbf{u}, \mathbf{v})$, $\bar{\mathbf{w}} = (\mathbf{w}, \mathbf{z})$ and

$$\begin{aligned} a(\bar{\mathbf{u}}, \bar{\mathbf{w}}) &= a_1(\mathbf{u}, \mathbf{w}) + a_2(\mathbf{v}, \mathbf{z}), \\ b(\bar{\mathbf{w}}, \mathbf{p}) &= b_1(\mathbf{w}, \mathbf{p}) + b_2(\mathbf{z}, \mathbf{p}), \\ c(\mathbf{p}, \mathbf{q}) &= a_3(\mathbf{p}, \mathbf{q}), \end{aligned}$$

with $a_1(\cdot, \cdot)$, $a_2(\cdot, \cdot)$, $a_3(\cdot, \cdot)$, $b_1(\cdot, \cdot)$ and $b_2(\cdot, \cdot)$ as defined in (3.3). Then, according to Theorem 5 in [26], for properly chosen seminorms $|\cdot|_{\mathbf{Q}}$ and $|\cdot|_{\bar{\mathbf{V}}}$, which are specified in Theorem 3.2 below, the uniform well-posedness of this problem is guaranteed under the fitted (full) norms

$$(3.7) \quad \|\mathbf{q}\|_{\bar{\mathbf{Q}}}^2 = |\mathbf{q}|_{\mathbf{Q}}^2 + c(\mathbf{q}, \mathbf{q}) =: \langle \bar{\mathbf{Q}}\mathbf{q}, \mathbf{q} \rangle_{\mathbf{Q}' \times \mathbf{Q}},$$

$$(3.8) \quad \|\bar{\mathbf{w}}\|_{\bar{\mathbf{V}}}^2 = |\bar{\mathbf{w}}|_{\bar{\mathbf{V}}}^2 + \langle B\bar{\mathbf{w}}, \bar{\mathbf{Q}}^{-1}B\bar{\mathbf{w}} \rangle_{\mathbf{Q}' \times \mathbf{Q}},$$

if the following two conditions are satisfied for positive constants c_a and c_b which are independent of all model parameters:

$$(3.9) \quad a(\bar{\mathbf{v}}, \bar{\mathbf{v}}) \geq c_a |\bar{\mathbf{v}}|_{\bar{\mathbf{V}}}^2, \quad \forall \bar{\mathbf{v}} \in \bar{\mathbf{V}},$$

$$(3.10) \quad \sup_{\bar{\mathbf{v}} \in \bar{\mathbf{V}}} \frac{b(\bar{\mathbf{v}}, \mathbf{q})}{\|\bar{\mathbf{v}}\|_{\bar{\mathbf{V}}}} \geq c_b |\mathbf{q}|_{\mathbf{Q}}, \quad \forall \mathbf{q} \in \mathbf{Q}.$$

This means that under the conditions (3.9) and (3.10) the bilinear form in (3.6) satisfies the estimates

$$(3.11) \quad |\mathcal{A}((\mathbf{u}, \mathbf{v}, \mathbf{p}), (\mathbf{w}, \mathbf{z}, \mathbf{q}))| \leq C_b \|(\mathbf{u}, \mathbf{v}, \mathbf{p})\|_{\bar{\mathbf{X}}} \|(\mathbf{w}, \mathbf{z}, \mathbf{q})\|_{\bar{\mathbf{X}}},$$

and

$$(3.12) \quad \inf_{(\mathbf{u}, \mathbf{v}, \mathbf{p}) \in \mathbf{X}} \sup_{(\mathbf{w}, \mathbf{z}, \mathbf{q}) \in \mathbf{X}} \frac{\mathcal{A}((\mathbf{u}, \mathbf{v}, \mathbf{p}), (\mathbf{w}, \mathbf{z}, \mathbf{q}))}{\|(\mathbf{u}, \mathbf{v}, \mathbf{p})\|_{\bar{\mathbf{X}}} \|(\mathbf{w}, \mathbf{z}, \mathbf{q})\|_{\bar{\mathbf{X}}}} \geq \omega,$$

for the combined norm $\|(\cdot, \cdot, \cdot)\|_{\bar{\mathbf{X}}}$ defined by

$$(3.13) \quad \|(\mathbf{w}, \mathbf{z}, \mathbf{q})\|_{\bar{\mathbf{X}}}^2 := \|\mathbf{q}\|_{\bar{\mathbf{Q}}}^2 + \|\bar{\mathbf{w}}\|_{\bar{\mathbf{V}}}^2$$

on the space $\mathbf{X} = \mathbf{U} \times \mathbf{V} \times \mathbf{P}$ with constants C_b and ω that do not depend on any of the model parameters.

Before we turn to the proof of estimates (3.11) and (3.12) in Theorem 3.2 below, we recall appropriate inf-sup conditions for the spaces \mathbf{U} , \mathbf{V} , \mathbf{P} in Lemma 3.1.

LEMMA 3.1. *The following conditions hold with constants $\beta_d > 0$ and $\beta_s > 0$:*

$$(3.14) \quad \inf_{q \in P_i} \sup_{\mathbf{v} \in \mathbf{V}_i} \frac{(\operatorname{div} \mathbf{v}, q)}{\|\mathbf{v}\|_1 \|q\|} \geq \beta_d, \quad i = 1, \dots, n,$$

$$(3.15) \quad \inf_{(q_1, \dots, q_n) \in P_1 \times \dots \times P_n} \sup_{\mathbf{u} \in U} \frac{\left(\operatorname{div} \mathbf{u}, \sum_{i=1}^n q_i \right)}{\|\mathbf{u}\|_1 \left\| \sum_{i=1}^n q_i \right\|} \geq \beta_s.$$

Proof. See [10, 9]. □

THEOREM 3.2. *Consider problem (3.2)–(3.3) on the space $\mathbf{X} = \mathbf{U} \times \mathbf{V} \times \mathbf{P} = \bar{\mathbf{V}} \times \mathbf{Q}$ and define the combined norm $\|\cdot\|_{\bar{\mathbf{X}}}$ via (3.13) where the fitted norms $\|\cdot\|_{\mathbf{Q}}$ and $\|\cdot\|_{\bar{\mathbf{V}}}$ are defined by (3.7)–(3.8) with seminorms*

$$(3.16) \quad |\mathbf{q}|_{\mathbf{Q}}^2 = ((\Lambda_3 + \Lambda_4)\mathbf{q}, \mathbf{q}),$$

$$(3.17) \quad |\bar{\mathbf{w}}|_{\bar{\mathbf{V}}}^2 = a(\bar{\mathbf{w}}, \bar{\mathbf{w}}).$$

Then, the continuity and stability estimates (3.11) and (3.12) hold with positive constants C_b and ω that are independent of all model parameters.

Proof. To prove statement (3.11), one uses the Cauchy-Schwarz inequality and the definition of the norms.

In order to prove (3.12) we verify the conditions of Theorem 5 in [26], i.e., conditions (3.9) and (3.10). Noting that $|\bar{\mathbf{w}}|_{\bar{\mathbf{V}}}^2 = a(\bar{\mathbf{w}}, \bar{\mathbf{w}})$, we find that condition (3.9) trivially holds with $c_a = 1$ so it remains to show (3.10). The bilinear form b is induced by the operator $B : \bar{\mathbf{V}} \rightarrow \mathbf{Q}'$ that is given by

$$B = \begin{pmatrix} -\alpha_1 \operatorname{div} & -\tau \operatorname{div} & 0 & 0 & \dots & 0 \\ -\alpha_2 \operatorname{div} & 0 & -\tau \operatorname{div} & 0 & \dots & 0 \\ -\alpha_3 \operatorname{div} & 0 & 0 & -\tau \operatorname{div} & \dots & 0 \\ \vdots & \vdots & \vdots & \vdots & \ddots & \vdots \\ -\alpha_n \operatorname{div} & 0 & 0 & 0 & \dots & -\tau \operatorname{div} \end{pmatrix}.$$

Thanks to Lemma 3.1, for a given $(\bar{\mathbf{u}}, \mathbf{p})$ we can choose test functions $\bar{\mathbf{w}} = (\mathbf{w}, \mathbf{z})$ such that

$$-\operatorname{div} \mathbf{w} = \frac{1}{2\mu + \lambda} \sum_{i=1}^n \alpha_i p_i, \quad \|\mathbf{w}\|_1 \leq \beta_s^{-1} \frac{1}{2\mu + \lambda} \left\| \sum_{i=1}^n \alpha_i p_i \right\|,$$

$$-\operatorname{div} \mathbf{z}_i = \tau R p_i, \quad \|\mathbf{z}_i\|_1 \leq \beta_s^{-1} \tau R \|p_i\|, \quad i = 1, \dots, n.$$

With these choices we find that

$$\begin{aligned} b(\bar{\mathbf{w}}, \mathbf{p}) &= -(\operatorname{div} \mathbf{w}, \sum_{i=1}^n \alpha_i p_i) - \sum_{i=1}^n (\tau \operatorname{div} \mathbf{z}_i, p_i) \\ &= \frac{1}{2\mu + \lambda} \left(\sum_{i=1}^n \alpha_i p_i, \sum_{i=1}^n \alpha_i p_i \right) + \sum_{i=1}^n (\tau^2 R p_i, p_i) \\ &= (\Lambda_4 \mathbf{p}, \mathbf{p}) + (\Lambda_3 \mathbf{p}, \mathbf{p}) = |\mathbf{p}|_{\mathbf{Q}}^2. \end{aligned}$$

In view of (3.8) and noting that $\langle B\bar{\mathbf{w}}, \bar{Q}^{-1}B\bar{\mathbf{w}} \rangle_{\mathbf{Q}' \times \mathbf{Q}} = (\Lambda^{-1}B\bar{\mathbf{w}}, \bar{\mathbf{w}})$, we obtain

$$\begin{aligned}
\|\bar{\mathbf{w}}\|_{\bar{\mathbf{V}}}^2 &= 2\mu(\varepsilon(\mathbf{w}), \varepsilon(\mathbf{w})) + \lambda(\operatorname{div} \mathbf{w}, \operatorname{div} \mathbf{w}) + \sum_{i=1}^n \gamma_i(\varepsilon(\mathbf{z}_i), \varepsilon(\mathbf{z}_i)) \\
&\quad + \sum_{i=1}^n (\tau K_i^{-1} \mathbf{z}_i, \mathbf{z}_i) + (\Lambda^{-1}B\bar{\mathbf{w}}, B\bar{\mathbf{w}}) \\
&\leq \beta_s^{-2} (2\mu + \lambda) \left(\frac{1}{2\mu + \lambda} \right)^2 \left\| \sum_{i=1}^n \alpha_i p_i \right\|^2 + \sum_{i=1}^n \gamma_i \beta_s^{-2} \tau^2 R^2 \|p_i\|^2 \\
&\quad + \sum_{i=1}^n \tau K_i^{-1} \beta_s^{-2} \tau^2 R^2 \|p_i\|^2 + (\Lambda^{-1}B\bar{\mathbf{w}}, B\bar{\mathbf{w}}) \\
&\leq \beta_s^{-2} \frac{1}{2\mu + \lambda} \left\| \sum_{i=1}^n \alpha_i p_i \right\|^2 + \beta_s^{-2} \sum_{i=1}^n (\gamma_i + \tau K_i^{-1}) \tau^2 R^2 \|p_i\|^2 + (\Lambda^{-1}B\bar{\mathbf{w}}, B\bar{\mathbf{w}}) \\
&\leq \beta_s^{-2} \frac{1}{2\mu + \lambda} \left\| \sum_{i=1}^n \alpha_i p_i \right\|^2 + \beta_s^{-2} \sum_{i=1}^n \tau^2 R \|p_i\|^2 + (\Lambda^{-1}B\bar{\mathbf{w}}, B\bar{\mathbf{w}}) \\
&\leq \beta_s^{-2} ((\Lambda_4 \mathbf{p}, \mathbf{p}) + (\Lambda_3 \mathbf{p}, \mathbf{p})) + ((\Lambda_3 + \Lambda_4)^{-1} B\bar{\mathbf{w}}, B\bar{\mathbf{w}}) \\
&\leq (\beta_s^{-2} + 1) |\mathbf{p}|_{\mathbf{Q}}^2,
\end{aligned}$$

where we have also used $(\Lambda^{-1}B\bar{\mathbf{w}}, B\bar{\mathbf{w}}) \leq ((\Lambda_3 + \Lambda_4)^{-1} B\bar{\mathbf{w}}, B\bar{\mathbf{w}})$ and $B\bar{\mathbf{w}} = (\Lambda_3 + \Lambda_4) \mathbf{p}$. Finally, (3.10) follows from

$$\sup_{\bar{\mathbf{v}} \in \bar{\mathbf{V}}} \frac{b(\bar{\mathbf{v}}, \mathbf{q})}{\|\bar{\mathbf{v}}\|_{\bar{\mathbf{V}}}} \geq \frac{b(\bar{\mathbf{w}}, \mathbf{q})}{\|\bar{\mathbf{w}}\|_{\bar{\mathbf{V}}}} \geq \frac{1}{\sqrt{\beta_s^{-2} + 1}} \frac{|\mathbf{q}|_{\mathbf{Q}}^2}{|\mathbf{q}|_{\mathbf{Q}}} = c_b |\mathbf{q}|_{\mathbf{Q}}, \quad \forall \mathbf{q} \in \mathbf{Q}. \quad \square$$

We have now established the well-posedness of the Biot-Brinkman problem under the specific combined norm $\|\cdot\|_{\bar{\mathbf{X}}}$ of the form (3.13), specified through (3.16) and (3.17). Next, we show that this combined norm is equivalent to the norm $\|\cdot\|_{\mathbf{X}}$ defined by

$$(3.18) \quad \|(\mathbf{w}, \mathbf{z}, \mathbf{q})\|_{\bar{\mathbf{X}}}^2 := \|\mathbf{w}\|_{\mathbf{U}}^2 + \|\mathbf{z}\|_{\bar{\mathbf{V}}}^2 + \|\mathbf{q}\|_{\mathbf{P}}^2.$$

The following Lemma is useful in establishing this norm equivalence, cf. [25, Lemma 2.1] where the statement has been proven for $\boldsymbol{\alpha} = (1, 1, \dots, 1)^T$.

LEMMA 3.3. *For any $a > 0$ and $b > 0$ and $\boldsymbol{\alpha} = (\alpha_1, \dots, \alpha_n)^T$, we have that*

$$(3.19) \quad (aI_{n \times n} + b\boldsymbol{\alpha}\boldsymbol{\alpha}^T)^{-1} = a^{-1}I - a^{-1}(ab^{-1} + \boldsymbol{\alpha}^T\boldsymbol{\alpha})^{-1}\boldsymbol{\alpha}\boldsymbol{\alpha}^T,$$

and

$$(3.20) \quad \boldsymbol{\alpha}^T (aI_{n \times n} + b\boldsymbol{\alpha}\boldsymbol{\alpha}^T)^{-1} \boldsymbol{\alpha} = \frac{\boldsymbol{\alpha}^T \boldsymbol{\alpha}}{ab^{-1} + \boldsymbol{\alpha}^T \boldsymbol{\alpha}} b^{-1} \leq b^{-1}.$$

Proof. The proof follows the lines of the proof of Lemma 2.1 in [25]. □

Now we can establish the following norm equivalence result.

LEMMA 3.4. *The norm (3.18) defined in terms of (2.12) is equivalent to the combined norm (3.13) based on (3.16) and (3.17).*

Proof. First, we note that

$$\begin{aligned} B\bar{\mathbf{w}} &= \begin{pmatrix} -\alpha_1 \operatorname{div} \mathbf{w} - \tau \operatorname{div} \mathbf{z}_1 \\ -\alpha_2 \operatorname{div} \mathbf{w} - \tau \operatorname{div} \mathbf{z}_2 \\ \vdots \\ -\alpha_n \operatorname{div} \mathbf{w} - \tau \operatorname{div} \mathbf{z}_n \end{pmatrix} = -\operatorname{div} \mathbf{w} \begin{pmatrix} \alpha_1 \\ \alpha_2 \\ \vdots \\ \alpha_n \end{pmatrix} + \tau \begin{pmatrix} -\operatorname{div} \mathbf{z}_1 \\ -\operatorname{div} \mathbf{z}_2 \\ \vdots \\ -\operatorname{div} \mathbf{z}_n \end{pmatrix} \\ &\equiv -\boldsymbol{\alpha} \operatorname{div} \mathbf{w} - \tau \operatorname{Div} \mathbf{z}. \end{aligned}$$

Then for any $1 > \epsilon > 0$, by Cauchy's inequality, we obtain

$$\begin{aligned} &(\Lambda^{-1} B\bar{\mathbf{w}}, B\bar{\mathbf{w}}) \\ &= (\Lambda^{-1} (\boldsymbol{\alpha} \operatorname{div} \mathbf{w} + \tau \operatorname{Div} \mathbf{z}), (\boldsymbol{\alpha} \operatorname{div} \mathbf{w} + \tau \operatorname{Div} \mathbf{z})) \\ &= (\Lambda^{-1} \boldsymbol{\alpha} \operatorname{div} \mathbf{w}, \boldsymbol{\alpha} \operatorname{div} \mathbf{w}) + 2(\Lambda^{-1} \boldsymbol{\alpha} \operatorname{div} \mathbf{w}, \tau \operatorname{Div} \mathbf{z}) + (\Lambda^{-1} \tau \operatorname{Div} \mathbf{z}, \tau \operatorname{Div} \mathbf{z}) \\ &\geq -(\epsilon^{-1} - 1)(\Lambda^{-1} \boldsymbol{\alpha} \operatorname{div} \mathbf{w}, \boldsymbol{\alpha} \operatorname{div} \mathbf{w}) + (1 - \epsilon)(\Lambda^{-1} \tau \operatorname{Div} \mathbf{z}, \tau \operatorname{Div} \mathbf{z}) \\ &\geq -(\epsilon^{-1} - 1)((\Lambda_3 + \Lambda_4)^{-1} \boldsymbol{\alpha} \operatorname{div} \mathbf{w}, \boldsymbol{\alpha} \operatorname{div} \mathbf{w}) + (1 - \epsilon)(\Lambda^{-1} \tau \operatorname{Div} \mathbf{z}, \tau \operatorname{Div} \mathbf{z}). \end{aligned}$$

By Lemma 3.3, with $a = \tau^2 R$, $b = \frac{1}{2\mu + \lambda}$, we have

$$\begin{aligned} &(\Lambda^{-1} B\bar{\mathbf{w}}, B\bar{\mathbf{w}}) \\ &\geq -(\epsilon^{-1} - 1)((\Lambda_3 + \Lambda_4)^{-1} \boldsymbol{\alpha} \operatorname{div} \mathbf{w}, \boldsymbol{\alpha} \operatorname{div} \mathbf{w}) + (1 - \epsilon)(\Lambda^{-1} \tau \operatorname{Div} \mathbf{z}, \tau \operatorname{Div} \mathbf{z}) \\ &= -(\epsilon^{-1} - 1)(\boldsymbol{\alpha}^T (\Lambda_3 + \Lambda_4)^{-1} \boldsymbol{\alpha} \operatorname{div} \mathbf{w}, \operatorname{div} \mathbf{w}) + (1 - \epsilon)(\Lambda^{-1} \tau \operatorname{Div} \mathbf{z}, \tau \operatorname{Div} \mathbf{z}) \\ &\geq -(\epsilon^{-1} - 1)(2\mu + \lambda)(\operatorname{div} \mathbf{w}, \operatorname{div} \mathbf{w}) + (1 - \epsilon)(\Lambda^{-1} \tau \operatorname{Div} \mathbf{z}, \tau \operatorname{Div} \mathbf{z}). \end{aligned}$$

Therefore, we get

$$\begin{aligned} \|\bar{\mathbf{w}}\|_{\mathbf{V}}^2 &= 2\mu(\varepsilon(\mathbf{w}), \varepsilon(\mathbf{w})) + \lambda(\operatorname{div} \mathbf{w}, \operatorname{div} \mathbf{w}) + \sum_{i=1}^n \gamma_i(\varepsilon(\mathbf{z}_i), \varepsilon(\mathbf{z}_i)) \\ &\quad + \sum_{i=1}^n (\tau K_i^{-1} \mathbf{z}_i, \mathbf{z}_i) + (\Lambda^{-1} B\bar{\mathbf{w}}, B\bar{\mathbf{w}}) \\ &\geq 2\mu(\varepsilon(\mathbf{w}), \varepsilon(\mathbf{w})) + \lambda(\operatorname{div} \mathbf{w}, \operatorname{div} \mathbf{w}) - (\epsilon^{-1} - 1)(2\mu + \lambda)(\operatorname{div} \mathbf{w}, \operatorname{div} \mathbf{w}) \\ &\quad + \sum_{i=1}^n \gamma_i(\varepsilon(\mathbf{z}_i), \varepsilon(\mathbf{z}_i)) + \sum_{i=1}^n (\tau K_i^{-1} \mathbf{z}_i, \mathbf{z}_i) + (1 - \epsilon)(\Lambda^{-1} \tau \operatorname{Div} \mathbf{z}, \tau \operatorname{Div} \mathbf{z}). \end{aligned}$$

Now, for $\epsilon = \frac{2}{3}$, we obtain

$$\begin{aligned} \|\bar{\mathbf{w}}\|_{\mathbf{V}}^2 &\geq 2\mu(\varepsilon(\mathbf{w}), \varepsilon(\mathbf{w})) + \lambda(\operatorname{div} \mathbf{w}, \operatorname{div} \mathbf{w}) - \frac{1}{2}(2\mu + \lambda)(\operatorname{div} \mathbf{w}, \operatorname{div} \mathbf{w}) \\ &\quad + \sum_{i=1}^n \gamma_i(\varepsilon(\mathbf{z}_i), \varepsilon(\mathbf{z}_i)) + \sum_{i=1}^n (\tau K_i^{-1} \mathbf{z}_i, \mathbf{z}_i) + \frac{1}{3}(\Lambda^{-1} \tau^2 \operatorname{Div} \mathbf{z}, \operatorname{Div} \mathbf{z}) \\ &\geq \frac{1}{2}(2\mu(\varepsilon(\mathbf{w}), \varepsilon(\mathbf{w})) + \lambda(\operatorname{div} \mathbf{w}, \operatorname{div} \mathbf{w})) \\ &\quad + \frac{1}{3} \left(\sum_{i=1}^n \gamma_i(\varepsilon(\mathbf{z}_i), \varepsilon(\mathbf{z}_i)) + \sum_{i=1}^n (\tau K_i^{-1} \mathbf{z}_i, \mathbf{z}_i) + (\Lambda^{-1} \tau^2 \operatorname{Div} \mathbf{z}, \operatorname{Div} \mathbf{z}) \right), \end{aligned}$$

namely $\|\mathbf{w}\|_{\mathbf{U}}^2 + \|\mathbf{z}\|_{\mathbf{V}}^2 \lesssim \|\bar{\mathbf{w}}\|_{\mathbf{V}}^2$. On the other hand, it is obvious that

$$\|\bar{\mathbf{w}}\|_{\mathbf{V}}^2 \lesssim \|\mathbf{w}\|_{\mathbf{U}}^2 + \|\mathbf{z}\|_{\mathbf{V}}^2.$$

Together, this gives $\|\bar{\mathbf{w}}\|_{\mathbf{V}}^2 \cong \|\mathbf{w}\|_{\mathbf{U}}^2 + \|\mathbf{z}\|_{\mathbf{V}}^2$. \square

In view of [Theorem 3.2](#) and [Lemma 3.4](#), we conclude that the Biot-Brinkman problem is also well-posed under the norm [\(3.18\)](#) defined in terms of [\(2.12\)](#). We summarize our results in the following theorem.

THEOREM 3.5.

(i) *There exists a positive constant C_b independent of the parameters $\lambda, K_i^{-1}, s_i, \beta_{ij}, i, j \in \{1, \dots, n\}$, the network scale n and the time step τ such that the inequality*

$$|\mathcal{A}((\mathbf{u}, \mathbf{v}, \mathbf{p}), (\mathbf{w}, \mathbf{z}, \mathbf{q}))| \leq C_b(\|\mathbf{u}\|_{\mathbf{U}} + \|\mathbf{v}\|_{\mathbf{V}} + \|\mathbf{p}\|_{\mathbf{P}})(\|\mathbf{w}\|_{\mathbf{U}} + \|\mathbf{z}\|_{\mathbf{V}} + \|\mathbf{q}\|_{\mathbf{P}})$$

holds true for any $(\mathbf{u}, \mathbf{v}, \mathbf{p}) \in \mathbf{U} \times \mathbf{V} \times \mathbf{P}, (\mathbf{w}, \mathbf{z}, \mathbf{q}) \in \mathbf{U} \times \mathbf{V} \times \mathbf{P}$.

(ii) *There is a constant $\omega > 0$ independent of the parameters $\lambda, K_i^{-1}, s_i, \beta_{ij}, i, j \in \{1, \dots, n\}$, the number of networks n and the time step τ such that*

$$\inf_{(\mathbf{u}, \mathbf{v}, \mathbf{p}) \in \mathbf{X}} \sup_{(\mathbf{w}, \mathbf{z}, \mathbf{q}) \in \mathbf{X}} \frac{\mathcal{A}((\mathbf{u}, \mathbf{v}, \mathbf{p}), (\mathbf{w}, \mathbf{z}, \mathbf{q}))}{(\|\mathbf{u}\|_{\mathbf{U}} + \|\mathbf{v}\|_{\mathbf{V}} + \|\mathbf{p}\|_{\mathbf{P}})(\|\mathbf{w}\|_{\mathbf{U}} + \|\mathbf{z}\|_{\mathbf{V}} + \|\mathbf{q}\|_{\mathbf{P}})} \geq \omega,$$

where $\mathbf{X} := \mathbf{U} \times \mathbf{V} \times \mathbf{P}$.

(iii) *The MPET system [\(3.4\)](#) has a unique solution $(\mathbf{u}, \mathbf{v}, \mathbf{p}) \in \mathbf{U} \times \mathbf{V} \times \mathbf{P}$ and the following stability estimate holds:*

$$\|\mathbf{u}\|_{\mathbf{U}} + \|\mathbf{v}\|_{\mathbf{V}} + \|\mathbf{p}\|_{\mathbf{P}} \leq C_1(\|\mathbf{f}\|_{\mathbf{U}'} + \|\mathbf{g}\|_{\mathbf{P}'}),$$

where C_1 is a positive constant independent of the parameters $\lambda, K_i^{-1}, s_i, \beta_{ij}, i, j \in \{1, \dots, n\}$, the network scale n and the time step τ , and $\|\mathbf{f}\|_{\mathbf{U}'} = \sup_{\mathbf{w} \in \mathbf{U}} \frac{(\mathbf{f}, \mathbf{w})}{\|\mathbf{w}\|_{\mathbf{U}}}, \|\mathbf{g}\|_{\mathbf{P}'} = \sup_{\mathbf{q} \in \mathbf{P}} \frac{(\mathbf{g}, \mathbf{q})}{\|\mathbf{q}\|_{\mathbf{P}}} = \|\Lambda^{-\frac{1}{2}} \mathbf{g}\|$.

4. Discrete generalized Biot-Brinkman problems. Stable and parameter-robust discretizations for the multiple network poroelasticity equations have been proposed based on a classical three-field formulation using a discontinuous Galerkin (DG) [\[1, 29\]](#) formulation of the momentum equation resulting in strong mass conservation, see [\[24\]](#), or based on a total pressure formulation in the setting of conforming methods in [\[36\]](#). These discrete models have been developed as generalizations of the corresponding Biot models, see [\[23\]](#) in case of conservative discretizations and [\[35\]](#) in case of the total pressure scheme. A hybridized version of the method in [\[23\]](#) has recently been presented in [\[33\]](#). For other conforming parameter-robust discretizations of the Biot model see also [\[15, 42\]](#) and [\[34\]](#), where the latter method is based on a total pressure formulation introducing the flux as a fourth field, which then also results in mass conservation. In this paper we extend the approach from [\[24, 23\]](#) to obtain mass-conservative discretizations for the generalized Biot-Brinkman system [\(3.2\)–\(3.3\)](#), which generalizes the MPET system.

4.1. Notation. Consider a shape-regular triangulation \mathcal{T}_h of the domain Ω into triangles/tetrahedrons, where the subscript h indicates the mesh-size. Following the standard notation, we first denote the set of all interior edges/faces and the set of all

boundary edges/faces of \mathcal{T}_h by \mathcal{E}_h^I and \mathcal{E}_h^B respectively, their union by \mathcal{E}_h and then we define the broken Sobolev spaces

$$H^s(\mathcal{T}_h) = \{\phi \in L^2(\Omega), \text{ such that } \phi|_T \in H^s(T) \text{ for all } T \in \mathcal{T}_h\}$$

for $s \geq 1$.

Next we introduce the notion of jumps $[\cdot]$ and averages $\{\cdot\}$ as follows. For any $q \in H^1(\mathcal{T}_h)$, $\mathbf{v} \in H^1(\mathcal{T}_h)^d$ and $\boldsymbol{\tau} \in H^1(\mathcal{T}_h)^{d \times d}$ and any $e \in \mathcal{E}_h^I$ the jumps are given as

$$[q] = q|_{\partial T_1 \cap e} - q|_{\partial T_2 \cap e}, \quad [\mathbf{v}] = \mathbf{v}|_{\partial T_1 \cap e} - \mathbf{v}|_{\partial T_2 \cap e}$$

and the averages as

$$\{\mathbf{v}\} = \frac{1}{2}(\mathbf{v}|_{\partial T_1 \cap e} \cdot \mathbf{n}_1 - \mathbf{v}|_{\partial T_2 \cap e} \cdot \mathbf{n}_2), \quad \{\boldsymbol{\tau}\} = \frac{1}{2}(\boldsymbol{\tau}|_{\partial T_1 \cap e} \mathbf{n}_1 - \boldsymbol{\tau}|_{\partial T_2 \cap e} \mathbf{n}_2),$$

while for $e \in \mathcal{E}_h^B$,

$$[q] = q|_e, \quad [\mathbf{v}] = \mathbf{v}|_e, \quad \{\mathbf{v}\} = \mathbf{v}|_e \cdot \mathbf{n}, \quad \{\boldsymbol{\tau}\} = \boldsymbol{\tau}|_e \mathbf{n}.$$

Here T_1 and T_2 are any two elements from the triangulation that share an edge or face e while \mathbf{n}_1 and \mathbf{n}_2 denote the corresponding unit normal vectors to e pointing to the exterior of T_1 and T_2 , respectively.

4.2. Mixed finite element spaces and discrete formulation. We consider the following finite element spaces to approximate the displacement, fluxes and pressures:

$$\mathbf{U}_h = \{\mathbf{u} \in H(\text{div}, \Omega) : \mathbf{u}|_T \in \mathbf{U}(T), T \in \mathcal{T}_h; \mathbf{u} \cdot \mathbf{n} = 0 \text{ on } \partial\Omega\},$$

$$\mathbf{V}_{i,h} = \{\mathbf{v} \in H(\text{div}, \Omega) : \mathbf{v}|_T \in \mathbf{V}_i(T), T \in \mathcal{T}_h; \mathbf{v} \cdot \mathbf{n} = 0 \text{ on } \partial\Omega\}, \quad i = 1, \dots, n,$$

$$P_{i,h} = \left\{ p \in L^2(\Omega) : p|_T \in P_i(T), T \in \mathcal{T}_h; \int_{\Omega} p dx = 0 \right\}, \quad i = 1, \dots, n,$$

where $\mathbf{U}(T)/\mathbf{V}_i(T)/P_i(T) = \text{BDM}_l(T)/\text{BDM}_l(T)/P_{l-1}(T)$ for $l \geq 1$. Note that for each of these choices $\text{div } \mathbf{U}(T) = \text{div } \mathbf{V}_i(T) = P_i(T)$ is fulfilled. We remark that the tangential part of the displacement boundary condition (2.9) is enforced by a Nitsche method, see e.g. [21]. Furthermore the orthogonality constraint for the pressures in $P_{i,h}$ is realized in the implementation by introducing (scalar) Lagrange multipliers.

Let us denote $\mathbf{v}_h^T = (\mathbf{v}_{1,h}^T, \dots, \mathbf{v}_{n,h}^T)$, $\mathbf{p}_h^T = (p_{1,h}, \dots, p_{n,h})$, $\mathbf{z}_h^T = (\mathbf{z}_{1,h}^T, \dots, \mathbf{z}_{n,h}^T)$, $\mathbf{q}_h^T = (q_{1,h}, \dots, q_{n,h})$ and

$$\mathbf{V}_h = \mathbf{V}_{1,h} \times \dots \times \mathbf{V}_{n,h}, \quad \mathbf{P}_h = P_{1,h} \times \dots \times P_{n,h}, \quad \mathbf{X}_h = \mathbf{U}_h \times \mathbf{V}_h \times \mathbf{P}_h.$$

The discretization of the variational problem (3.2)–(3.3) now is given as follows: find $(\mathbf{u}_h, \mathbf{v}_h, \mathbf{p}_h) \in \mathbf{X}_h$, such that for any $(\mathbf{w}_h, \mathbf{z}_h, \mathbf{q}_h) \in \mathbf{X}_h$ and $i = 1, \dots, n$

$$(4.1a) \quad a_h(\mathbf{u}_h, \mathbf{w}_h) + \lambda(\text{div } \mathbf{u}_h, \text{div } \mathbf{w}_h) + (\boldsymbol{\alpha} \cdot \mathbf{p}_h, \text{div } \mathbf{w}_h) = (\mathbf{f}, \mathbf{w}_h),$$

$$(4.1b) \quad \gamma_i a_h(\mathbf{v}_{i,h}, \mathbf{z}_{i,h}) + (\tau K_i^{-1} \mathbf{v}_{i,h}, \mathbf{z}_{i,h}) + (p_{i,h}, \tau \text{div } \mathbf{z}_{i,h}) = 0, \\ (\text{div } \mathbf{u}_h, \alpha_i q_{i,h}) + (\tau \text{div } \mathbf{v}_{i,h}, q_{i,h}) - s_i(p_{i,h}, q_{i,h})$$

$$(4.1c) \quad + \sum_{j=1}^n \tau \beta_{ij} (p_{j,h}, q_{i,h}) = (g_i, q_{i,h}),$$

where

$$(4.2) \quad \begin{aligned} a_h(\phi, \psi) &= \sum_{T \in \mathcal{T}_h} \int_T \boldsymbol{\varepsilon}(\phi) : \boldsymbol{\varepsilon}(\psi) \, dx - \sum_{e \in \mathcal{E}_h} \int_e \{\boldsymbol{\varepsilon}(\phi)\} \cdot [\boldsymbol{\psi}_t] \, ds \\ &\quad - \sum_{e \in \mathcal{E}_h} \int_e \{\boldsymbol{\varepsilon}(\psi)\} \cdot [\phi_t] \, ds + \sum_{e \in \mathcal{E}_h} \int_e \eta h_e^{-1} [\phi_t] \cdot [\boldsymbol{\psi}_t] \, ds, \end{aligned}$$

and η is a stabilization parameter independent of all other problem parameters, the network scale n and the mesh size h .

We note that the discrete variational problem (4.1) has been derived for the weak formulation (3.4) with homogeneous boundary conditions. For general rescaled boundary conditions with DG discretizations we refer the reader to e.g. [23].

4.3. Stability properties. For any function $\phi \in \mathbf{H}^2(\mathcal{T}_h) := H^2(\mathcal{T}_h)^d$, consider the following mesh dependent norms

$$\begin{aligned} \|\phi\|_h^2 &= \sum_{T \in \mathcal{T}_h} \|\boldsymbol{\varepsilon}(\phi)\|_T^2 + \sum_{e \in \mathcal{E}_h} h_e^{-1} \|[\phi_t]\|_e^2, \\ \|\phi\|_{1,h}^2 &= \sum_{T \in \mathcal{T}_h} \|\nabla \phi\|_T^2 + \sum_{e \in \mathcal{E}_h} h_e^{-1} \|[\phi_t]\|_e^2, \end{aligned}$$

and

$$(4.3) \quad \|\phi\|_{DG}^2 = \sum_{T \in \mathcal{T}_h} \|\nabla \phi\|_T^2 + \sum_{e \in \mathcal{E}_h} h_e^{-1} \|[\phi_t]\|_e^2 + \sum_{T \in \mathcal{T}_h} h_T^2 |\phi|_{2,T}^2.$$

Details about the well-posedness and approximation properties of the DG formulation of elasticity, Stokes and Brinkman-type systems can be found in [28, 22].

Now, for $\mathbf{u} \in H(\operatorname{div}, \Omega) \cap \mathbf{H}^2(\mathcal{T}_h)$, we define the norm

$$(4.4) \quad \|\mathbf{u}\|_{\mathbf{U}_h}^2 = \|\mathbf{u}\|_{DG}^2 + \lambda \|\operatorname{div} \mathbf{u}\|^2$$

and for $\mathbf{v} \in H(\operatorname{div}, \Omega) \cap \mathbf{H}^2(\mathcal{T}_h)$, we define the norm

$$(4.5) \quad \|\mathbf{v}\|_{\mathbf{V}_h}^2 = \sum_{i=1}^n (\gamma_i \|\mathbf{v}_i\|_{DG}^2 + (\tau K_i^{-1} \mathbf{v}_i, \mathbf{v}_i)) + (\Lambda^{-1} \operatorname{Div} \mathbf{v}, \operatorname{Div} \mathbf{v}).$$

The well-posedness and approximation properties of the DG formulation are detailed in [28, 22]. Here we briefly present some important results:

- $\|\cdot\|_{DG}$, $\|\cdot\|_h$, and $\|\cdot\|_{1,h}$ are equivalent on \mathbf{U}_h ; that is

$$\|\mathbf{u}_h\|_{DG} \approx \|\mathbf{u}_h\|_h \approx \|\mathbf{u}_h\|_{1,h}, \text{ for all } \mathbf{u}_h \in \mathbf{U}_h.$$

- a_h from (4.2) is continuous and it holds true that

$$(4.6) \quad |a_h(\mathbf{u}, \mathbf{w})| \lesssim \|\mathbf{u}\|_{DG} \|\mathbf{w}\|_{DG}, \text{ for all } \mathbf{u}, \mathbf{w} \in \mathbf{H}^2(\mathcal{T}_h).$$

- The following inf-sup conditions are satisfied

$$(4.7) \quad \begin{aligned} \inf_{(q_{1,h}, \dots, q_{n,h}) \in P_{1,h} \times \dots \times P_{n,h}} \sup_{\mathbf{u}_h \in \mathbf{U}_h} \frac{(\operatorname{div} \mathbf{u}_h, \sum_{i=1}^n q_{i,h})}{\|\mathbf{u}_h\|_{1,h} \sum_{i=1}^n \|q_{i,h}\|} &\geq \beta_{sd}, \\ \inf_{q_{i,h} \in P_{i,h}} \sup_{\mathbf{v}_{i,h} \in \mathbf{V}_{i,h}} \frac{(\operatorname{div} \mathbf{v}_{i,h}, q_{i,h})}{\|\mathbf{v}_{i,h}\|_{1,h} \|q_{i,h}\|} &\geq \beta_{dd}, \quad i = 1, \dots, n. \end{aligned}$$

Using the definition of the matrices Λ_1 and Λ_2 , next we define the bilinear form

$$\begin{aligned}
 \mathcal{A}_h((\mathbf{u}_h, \mathbf{v}_h, \mathbf{p}_h), (\mathbf{w}_h, \mathbf{z}_h, \mathbf{q}_h)) &= a_h(\mathbf{u}_h, \mathbf{w}_h) + \lambda(\operatorname{div} \mathbf{u}_h, \operatorname{div} \mathbf{w}_h) \\
 &+ \sum_{i=1}^n (\alpha_i p_{i,h}, \operatorname{div} \mathbf{w}_h) + \sum_{i=1}^n \gamma_i a_h(\mathbf{v}_{i,h}, \mathbf{z}_{i,h}) \\
 (4.8) \quad &+ \sum_{i=1}^n (\tau K_i^{-1} \mathbf{v}_{i,h}, \mathbf{z}_{i,h}) + \tau(\mathbf{p}_h, \operatorname{Div} \mathbf{z}_h) \\
 &+ \sum_{i=1}^n (\operatorname{div} \mathbf{u}_h, \alpha_i q_{i,h}) + \tau(\operatorname{Div} \mathbf{v}_h, \mathbf{q}_h) - ((\Lambda_1 + \Lambda_2) \mathbf{p}_h, \mathbf{q}_h)
 \end{aligned}$$

related to problem (4.1a)–(4.1c).

We equip \mathbf{X}_h with the norm defined by $\|(\cdot, \cdot, \cdot)\|_{\mathbf{X}_h}^2 := \|\cdot\|_{\mathbf{U}_h}^2 + \|\cdot\|_{\mathbf{V}_h}^2 + \|\cdot\|_{\mathbf{P}}^2$. Similar to Theorem 3.5, the following uniform stability result holds:

THEOREM 4.1.

(i) For any $\mathbf{u}_h, \mathbf{w}_h \in \mathbf{U}_h$; $\mathbf{v}_h, \mathbf{z}_h \in \mathbf{V}_h$; $\mathbf{p}_h, \mathbf{q}_h \in \mathbf{P}_h$ there exists a positive constant C_{bd} independent of all model parameters, the network scale n and the mesh size h such that the inequality

$$|\mathcal{A}_h((\mathbf{u}_h, \mathbf{v}_h, \mathbf{p}_h), (\mathbf{w}_h, \mathbf{z}_h, \mathbf{q}_h))| \leq C_{bd} \|(\mathbf{u}_h, \mathbf{v}_h, \mathbf{p}_h)\|_{\mathbf{X}_h} \|(\mathbf{w}_h, \mathbf{z}_h, \mathbf{q}_h)\|_{\mathbf{X}_h}$$

holds true.

(ii) There exists a constant $\omega_d > 0$ independent of all discretization and model parameters such that

$$(4.9) \quad \inf_{(\mathbf{u}_h, \mathbf{v}_h, \mathbf{p}_h) \in \mathbf{X}_h} \sup_{(\mathbf{w}_h, \mathbf{z}_h, \mathbf{q}_h) \in \mathbf{X}_h} \frac{\mathcal{A}_h((\mathbf{u}_h, \mathbf{v}_h, \mathbf{p}_h), (\mathbf{w}_h, \mathbf{z}_h, \mathbf{q}_h))}{\|(\mathbf{u}_h, \mathbf{v}_h, \mathbf{p}_h)\|_{\mathbf{X}_h} \|(\mathbf{w}_h, \mathbf{z}_h, \mathbf{q}_h)\|_{\mathbf{X}_h}} \geq \omega_d.$$

(iii) Let $(\mathbf{u}_h, \mathbf{v}_h, \mathbf{p}_h) \in \mathbf{X}_h$ solve (4.1a)–(4.1c) and

$$\|\mathbf{f}\|_{\mathbf{U}'_h} = \sup_{\mathbf{w}_h \in \mathbf{U}_h} \frac{(\mathbf{f}, \mathbf{w}_h)}{\|\mathbf{w}_h\|_{\mathbf{U}_h}}, \quad \|\mathbf{g}\|_{\mathbf{P}'} = \sup_{\mathbf{q}_h \in \mathbf{P}_h} \frac{(\mathbf{g}, \mathbf{q}_h)}{\|\mathbf{q}_h\|_{\mathbf{P}}}.$$

Then the estimate

$$\|\mathbf{u}_h\|_{\mathbf{U}_h} + \|\mathbf{v}_h\|_{\mathbf{V}_h} + \|\mathbf{p}_h\|_{\mathbf{P}} \leq C_2 (\|\mathbf{f}\|_{\mathbf{U}'_h} + \|\mathbf{g}\|_{\mathbf{P}'})$$

holds with a constant C_2 independent of the network scale n , the mesh size h , the time step τ and the parameters λ , K_i^{-1} , s_i , β_{ij} , $i, j \in \{1, \dots, n\}$.

4.4. Error estimates. This subsection summarizes the error estimates that follow from the stability results presented in Subsection 4.3.

THEOREM 4.2. Assume that $(\mathbf{u}, \mathbf{v}, \mathbf{p}) \in \mathbf{U} \cap \mathbf{H}^2(\mathcal{T}_h) \times \mathbf{V} \cap \mathbf{H}^2(\mathcal{T}_h) \times \mathbf{P}$ is the unique solution of (3.2)–(3.3), and let $(\mathbf{u}_h, \mathbf{v}_h, \mathbf{p}_h)$ be the solution of (4.1). Then the error estimates

$$(4.10) \quad \|\mathbf{u} - \mathbf{u}_h\|_{\mathbf{U}_h} + \|\mathbf{v} - \mathbf{v}_h\|_{\mathbf{V}_h} \lesssim \inf_{\mathbf{w}_h \in \mathbf{U}_h, \mathbf{z}_h \in \mathbf{V}_h} \left(\|\mathbf{u} - \mathbf{w}_h\|_{\mathbf{U}_h} + \|\mathbf{v} - \mathbf{z}_h\|_{\mathbf{V}_h} \right),$$

$$(4.11) \quad \|\mathbf{p} - \mathbf{p}_h\|_{\mathbf{P}} \lesssim \inf_{\mathbf{w}_h \in \mathbf{U}_h, \mathbf{z}_h \in \mathbf{V}_h, \mathbf{q}_h \in \mathbf{P}_h} \left(\|\mathbf{u} - \mathbf{w}_h\|_{\mathbf{U}_h} + \|\mathbf{v} - \mathbf{z}_h\|_{\mathbf{V}_h} + \|\mathbf{p} - \mathbf{q}_h\|_{\mathbf{P}} \right),$$

hold true, where the inequality constants are independent of the parameters λ , K_i^{-1} , s_i , β_{ij} for $i, j = 1, \dots, n$, the network scale n , the mesh size h and the time step τ .

Proof. The proof of this result is analogous to the proof of Theorem 5.2 in [23]. \square

Remark 4.3. In particular, the above theorem shows that the proposed discretizations are locking-free. Note that estimate (4.10) controls the error in \mathbf{u} plus the error in \mathbf{v} by the sum of the errors of the corresponding best approximations whereas estimate (4.11) requires the best approximation errors of all three vector variables \mathbf{u} , \mathbf{v} and \mathbf{p} to control the error in \mathbf{p} .

4.5. A norm equivalent preconditioner. We consider the following block-diagonal operator

$$(4.12) \quad \mathcal{B} := \begin{bmatrix} \mathcal{B}_u & \mathbf{0} & \mathbf{0} \\ \mathbf{0} & \mathcal{B}_v & \mathbf{0} \\ \mathbf{0} & \mathbf{0} & \mathcal{B}_p \end{bmatrix}^{-1},$$

where

$$\mathcal{B}_u = -\operatorname{div} \boldsymbol{\varepsilon} - \lambda \nabla \operatorname{div},$$

$$\mathcal{B}_v = \begin{bmatrix} -\gamma_1 \operatorname{div} \boldsymbol{\varepsilon} + \tau K_1^{-1} I & 0 & \dots & 0 \\ 0 & -\gamma_2 \operatorname{div} \boldsymbol{\varepsilon} + \tau K_2^{-1} I & \dots & 0 \\ \vdots & \vdots & \ddots & \vdots \\ 0 & 0 & \dots & -\gamma_n \operatorname{div} \boldsymbol{\varepsilon} + \tau K_n^{-1} I \end{bmatrix}$$

$$- \begin{bmatrix} \tilde{\Lambda}_{11} \nabla \operatorname{div} & \tilde{\Lambda}_{12} \nabla \operatorname{div} & \dots & \tilde{\Lambda}_{1n} \nabla \operatorname{div} \\ \tilde{\Lambda}_{21} \nabla \operatorname{div} & \tilde{\Lambda}_{22} \nabla \operatorname{div} & \dots & \tilde{\Lambda}_{2n} \nabla \operatorname{div} \\ \vdots & \vdots & \ddots & \vdots \\ \tilde{\Lambda}_{n1} \nabla \operatorname{div} & \tilde{\Lambda}_{n2} \nabla \operatorname{div} & \dots & \tilde{\Lambda}_{nn} \nabla \operatorname{div} \end{bmatrix}$$

and

$$\mathcal{B}_p = \begin{bmatrix} \Lambda_{11} I & \Lambda_{12} I & \dots & \Lambda_{1n} I \\ \Lambda_{21} I & \Lambda_{22} I & \dots & \Lambda_{2n} I \\ \vdots & \vdots & \ddots & \vdots \\ \Lambda_{n1} I & \Lambda_{n2} I & \dots & \Lambda_{nn} I \end{bmatrix}.$$

Here, Λ_{ij} , $\tilde{\Lambda}_{ij}$, $i, j = 1, \dots, n$ are the entries of Λ and Λ^{-1} , respectively.

As substantiated in [24], the stability results for the operator \mathcal{A} in (3.5) imply that the operator \mathcal{B} is a uniform norm-equivalent (canonical) block-diagonal preconditioner that is robust with respect to all model and discretization parameters. Note that \mathcal{B} defines a canonical uniform block-diagonal preconditioner on the continuous as well as on the discrete level as long as discrete inf-sup conditions analogous to (3.14) and (3.15) are satisfied, cf. [24].

5. Numerical experiments. In this section we present numerical experiments whose results corroborate stability properties of the finite element discretization of the generalized Biot-Brinkman model (see Subsection 4.4) and the preconditioner (4.12). We shall first demonstrate parameter robustness of the exact preconditioner through a sensitivity study of the conditioning of the preconditioned Biot-Brinkman system. Afterwards, scalable realization of the preconditioner in terms multilevel methods for the displacement and flux blocks is discussed. For simplicity, all the experiments concern the domain $\Omega = (0, 1)^2$. The implementation was carried in the Firedrake finite element framework [41].

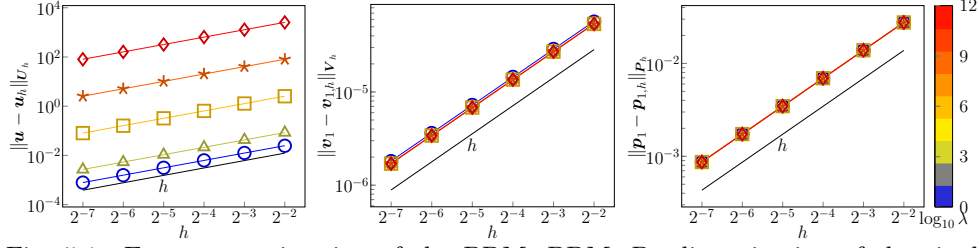


Fig. 5.1: Error approximation of the $\text{BDM}_1\text{-BDM}_1\text{-P}_0$ discretization of the single network Biot-Brinkman model. Parameters $\mu = 1$, $\tau = 10^{-1}$, $\alpha_1 = 10^{-3}$, $c_1 = 10^{-2}$, $\nu_1 = 1$ and $K_1 = 1$ are fixed. Line colors correspond to different values of λ .

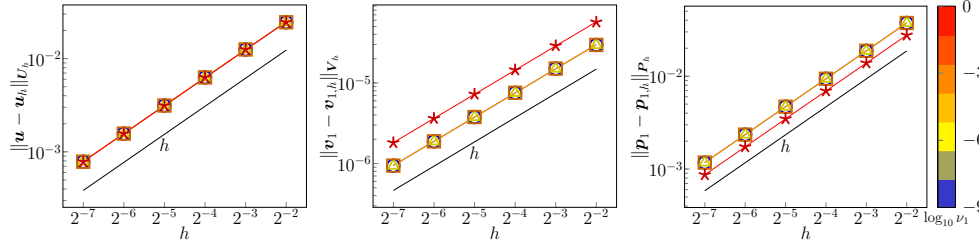


Fig. 5.2: Error approximation of the $\text{BDM}_1\text{-BDM}_1\text{-P}_0$ discretization of the single network Biot-Brinkman model. Parameters $\mu = 1$, $\tau = 10^{-1}$, $\alpha_1 = 10^{-3}$, $c_1 = 10^{-2}$, $K_1 = 1$ and $\lambda = 1$ are fixed. Line colors correspond to different values of ν_1 .

5.1. Error estimates. We consider a single network, $n = 1$, case of the generalized Biot-Brinkman model (3.5), with parameters $\mu = 1$, $\tau = 10^{-1}$, $\alpha_1 = 10^{-3}$ and $c_1 = 10^{-2}$ fixed (arbitrarily) while K_1 , ν_1 and λ shall be varied in order to test robustness of the error estimates established in Subsection 4.4. To this end, we solve (2.8) with the right hand side computed based on the exact solution

$$(5.1) \quad \mathbf{u} = \begin{pmatrix} \frac{\partial \phi}{\partial y} \\ -\frac{\partial \phi}{\partial x} \end{pmatrix}, \quad \mathbf{v}_1 = \nabla \phi_1, \quad p_1 = \sin \pi(x - y),$$

where

$$\phi = x^2(x-1)^2y^2(y-1)^2, \quad \phi_1 = x^4(x-1)^4y^4(y-1)^4.$$

It can be seen that the manufactured solution satisfies the homogeneous conditions $\mathbf{u}|_{\partial\Omega} = \mathbf{0}$, $\mathbf{v}_1 \cdot \mathbf{n}|_{\partial\Omega} = 0$ for $\Omega = (0, 1)^2$.

Using discretization by BDM_1 elements for \mathbf{U}_h , $\mathbf{V}_{1,h}$ and piece-wise constant elements for the pressure space $P_{1,h}$, Figure 5.1–Figure 5.3 show the errors of the numerical approximations in the parameter-dependent norms (4.4), (4.5) and $\|\cdot\|_{\mathcal{P}}$ defined in (2.12c) when one of the parameters λ , K_1 and ν_1 is varied. In all the cases the expected linear convergence can be observed. In particular, the rate is independent of the parameter variations. We note that the error here is computed on a finer mesh than the finite element solution in order to prevent aliasing.

5.2. Robustness of exact preconditioner. We verify robustness of the canonical preconditioner (4.12) using a generalized Biot-Brinkman system with two networks. As the parameter space then counts 12 parameters in total we shall for simplicity fix material properties of one of the networks (below we choose the network

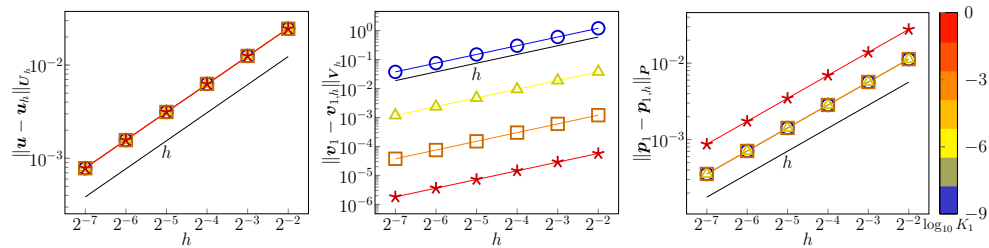


Fig. 5.3: Error approximation of the BDM₁-BDM₁-P₀ discretization of the single network Biot-Brinkman model. Parameters $\mu = 1$, $\tau = 10^{-1}$, $\alpha_1 = 10^{-3}$, $c_1 = 10^{-2}$, $\nu_1 = 1$ and $\lambda = 1$ are fixed. Line colors correspond to different values of K_1 .

$i = 1$) to unity in addition to setting $\mu = 1$, $\tau = 1$. This choice leaves parameters λ , c_2 , α_2 , ν_2 , K_2 as well as the transfer coefficient $\beta := \beta_{12}$ to be varied. In the following experiments we let $1 \leq \lambda \leq 10^{12}$, $10^{-9} \leq \nu_2, K_2, \alpha_2 \leq 1$, $10^{-6} \leq \beta \leq 10^6$ and $c_2 \in \{0, 1\}$ in order to perform a systematic sensitivity study. We note that we do not vary directly the scaling parameters introduced in (3.5) but instead change the material parameters in (1.1).

For the above choice of parameters the two-network problem is considered on the domain $\Omega = (0, 1)^2$ with boundary conditions $\mathbf{u} = \mathbf{0}$ on the left and right sides and $(\boldsymbol{\sigma} + \boldsymbol{\alpha} \cdot \mathbf{p}\mathbf{I}) \cdot \mathbf{n} = \mathbf{0}$ on the remaining part of the boundary; similarly, the Dirichlet conditions $\mathbf{v}_i \cdot \mathbf{n} = 0$, $i = 1, 2$ on the fluxes are prescribed only on the left and right sides.

Having constructed spaces \mathbf{U}_h , $\mathbf{V}_{1,h}$, $\mathbf{V}_{2,h}$ with BDM₁ elements and pressure spaces $P_{1,h}$, $P_{2,h}$ in terms of piece-wise constants our results are summarized in Figure 5.4–Figure 5.6 where slices of the explored parameter space are shown. It can be seen that the condition numbers remain bounded. Concretely, given discrete operators \mathcal{A}_h , \mathcal{B}_h that respectively discretize (3.5) and the preconditioner (4.12) the condition number is computed based on the generalized eigenvalue problem $\mathcal{A}_h x_k = \lambda_k \mathcal{B}_h^{-1} x_k$ as $\max_k |\lambda_k| / \min_k |\lambda_k|$. The higher condition numbers (of about 8.5) are typically attained when $c_2 = 0$, $\lambda = 1$ and $\beta \ll 1$. We remark that with $c_2 = 0$ and all parameters but β set to 1 the condition number of Λ ranges from 2.64 when $\beta = 10^{-6}$ to about 10^6 when $\beta = 10^6$.

5.3. Multigrid preconditioning. Having seen that the exact preconditioner (4.12) yields parameter-robustness let us next discuss possible construction of a scalable approximation of the operator \mathcal{B} . Here, in order to approximate \mathcal{B}_u and \mathcal{B}_v , we follow [22, 2, 19] and employ vertex-star relaxation schemes as part of geometric multigrid $F(2, 2)$ -cycle for the elastic block and $W(2, 2)$ -cycle for the flux block. Numerical experiments documenting robustness of the cycles for their respective blocks are reported in Appendix A.

To test performance of the multigrid-based preconditioner \mathcal{B} we consider the two-network system from Subsection 5.2 where we set $c_2 = 0$, $\alpha_2 = 1$, $\beta \in \{10^{-6}, 10^6\}$ while the remaining parameters are fixed to unity. We remark that for these parameter values the highest condition numbers are attained with the exact preconditioner, cf. Figure 5.4. Furthermore, differing from the setup of the sensitivity study, we (strongly) enforce $\mathbf{u} \cdot \mathbf{n} = 0$ and $\mathbf{v}_i \cdot \mathbf{n} = 0$, $i = 1, 2$, on the entire boundary¹. As

¹The reason for not prescribing the complete displacement vector as a boundary condition are

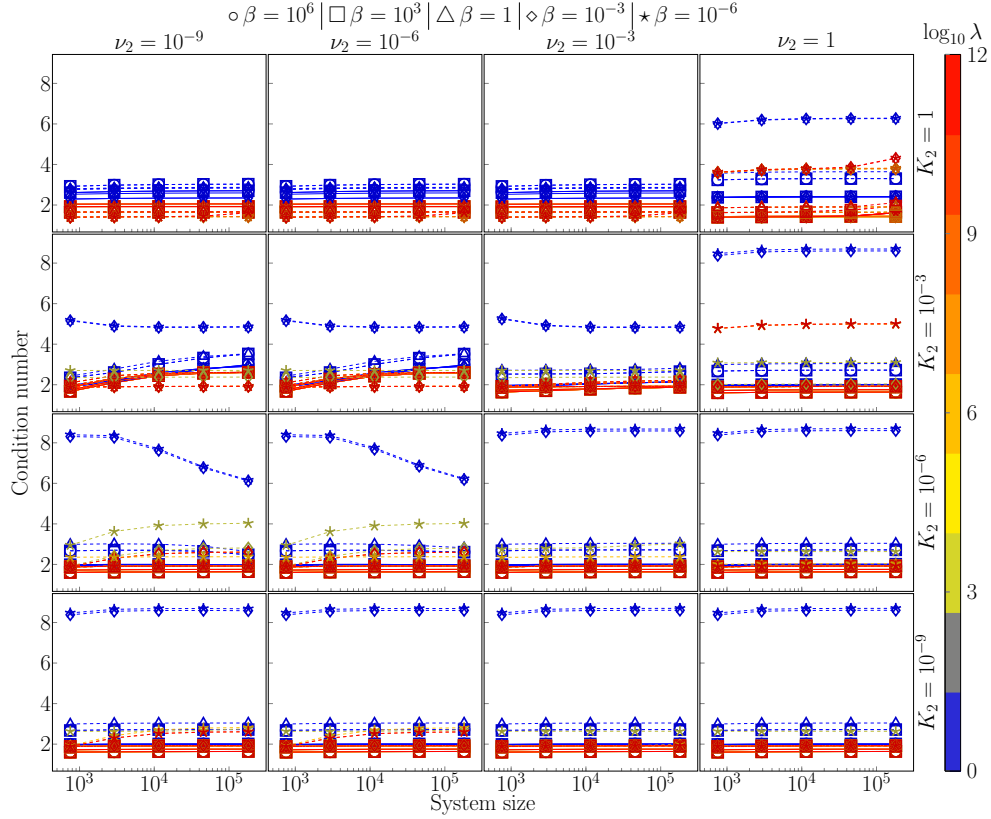


Fig. 5.4: Performance of Biot-Brinkman preconditioner (4.12) for $\alpha_2 = 1$ and varying parameters λ , ν_2 , K_2 , β (denoted by markers). Binary storage capacity is considered: $c_2 = 1$ (solid lines), $c_2 = 0$ (dashed lines). The remaining parameters are fixed at 1. Discretization by BDM_1 - $(\text{BDM}_1)^2$ - $(\text{P}_0)^2$ elements. Highest condition numbers correspond to $\beta \ll 1$ and $c_2 = 0$, $\lambda = 1$.

before, the finite element discretization is based on the BDM_1 and P_0 elements.

In Figure 5.7 and Figure 5.8 we report the dependence on the mesh size and parameter values of the iteration counts of the preconditioned MinRes solver where as the preconditioner both the exact Riesz map (4.12) and the multigrid-based approximation are used. More specifically, the multigrid cycles for the displacement and flux blocks use 3 grid levels applying the exact L^2 -projection as the transfer operator. For both \mathcal{B}_u and \mathcal{B}_v the vertex-star relaxation uses damped Richardson smoother. Comparing the results we observe that the use of multigrid in (4.12) translates to a slight (about 1.5x) increase in the number of Krylov iterations compared to the exact preconditioner. However, the iterations appear bounded in the mesh size and the parameter variations.

We finally compare the cost of the exact and inexact Biot-Brinkman precondi-

limitations in the PCPATCH framework which was used to implement the multigrid algorithm. In particular, the software currently lacks support for exterior facet integrals (see e.g. [3]) which are required with BDM elements to weakly enforce conditions on the tangential displacement by the Nitsche method.

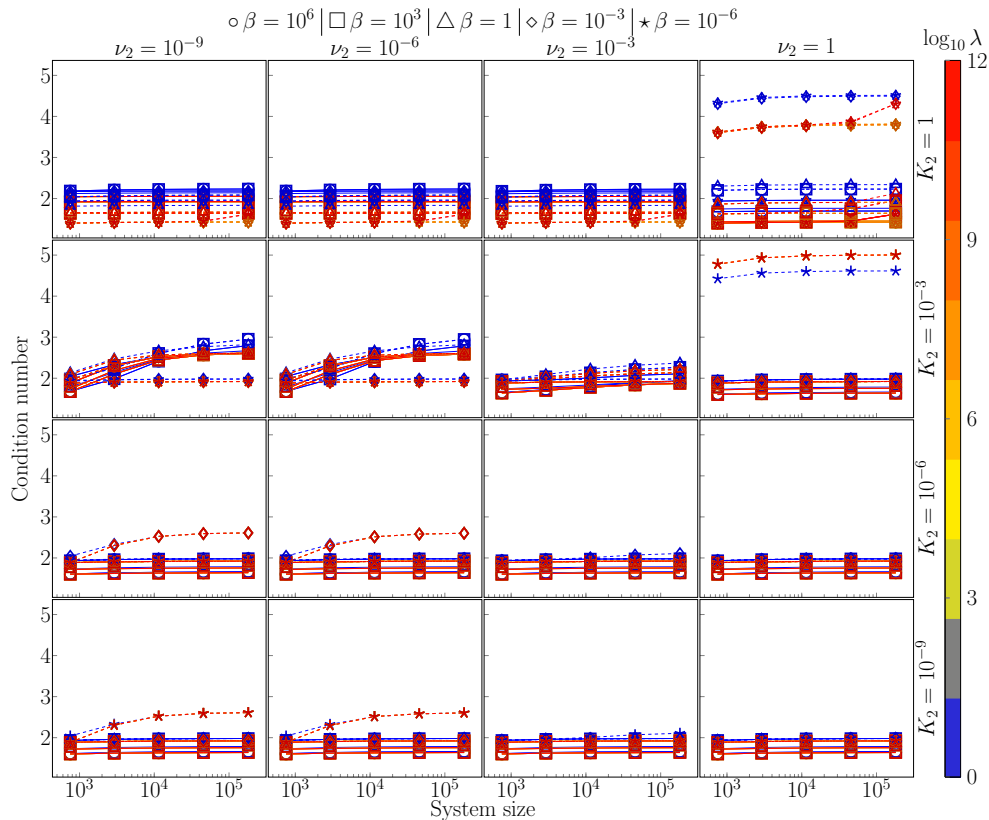


Fig. 5.5: Performance of Biot-Brinkman preconditioner (4.12) for $\alpha_2 = 10^{-4}$ and varying parameters λ , ν_2 , K_2 , β (denoted by markers). Binary storage capacity is considered: $c_2 = 1$ (solid lines), $c_2 = 0$ (dashed lines). The remaining parameters are fixed at 1. Discretization by BDM_1 - $(\text{BDM}_1)^2$ - $(\text{P}_0)^2$ elements.

tioners for case $K_2 = 10^{-3}$, $\lambda = 1$, $\beta = 10^{-6}$ which required most iterations in the previous experiments, cf. Figure 5.8. Our results are summarized in Table 5.1. We observe that despite requiring more iterations for convergence the solution time² with the multigrid-based preconditioner is noticeably faster. In addition, the resulting solution algorithm appears to scale linearly in the number of unknowns. We remark that for the sake of simple comparison the computations were done in serial using single-threaded execution. However, the latter setting is particularly unfavorable for the exact preconditioner \mathcal{B} as modern LU solvers are known for their thread efficiency.

REFERENCES

- [1] D. N. ARNOLD, F. BREZZI, B. COCKBURN, AND L. D. MARINI, *Unified analysis of discontinuous Galerkin methods for elliptic problems*, SIAM journal on numerical analysis, 39 (2002), pp. 1749–1779.

²The comparison is done in terms of the aggregate of the setup time of the preconditioner and the run time of the Krylov solver.

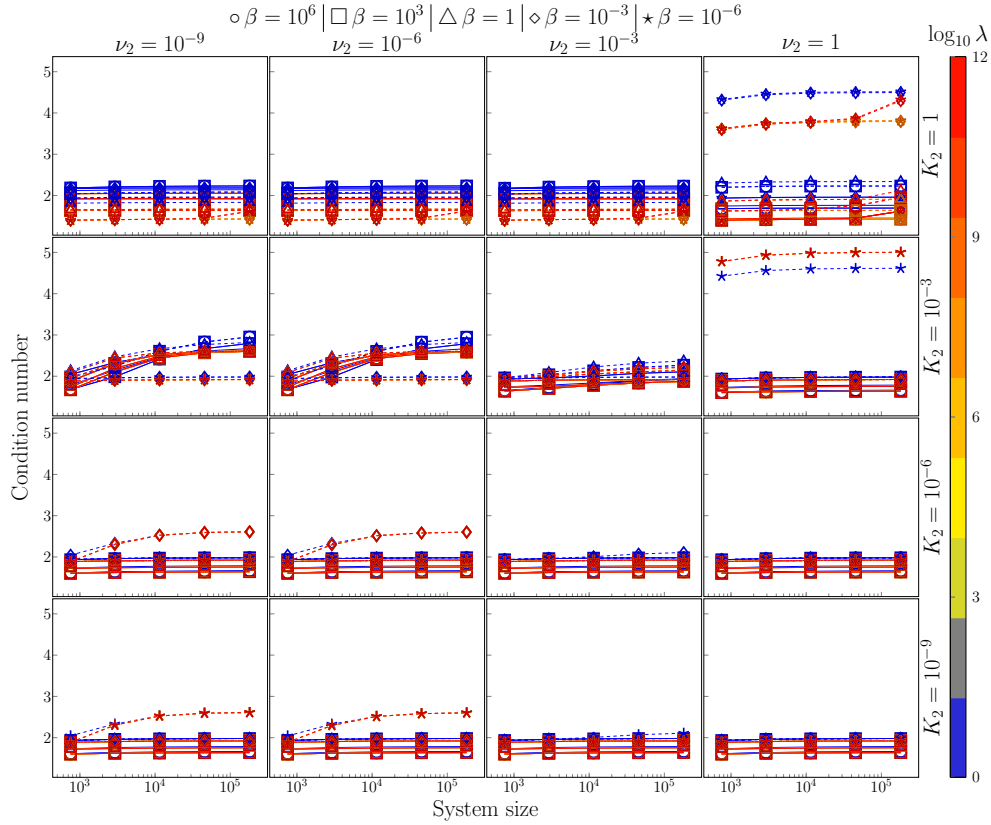


Fig. 5.6: Performance of Biot-Brinkman preconditioner (4.12) for $\alpha_2 = 10^{-8}$ and varying parameters λ , ν_2 , K_2 , β (denoted by markers). Binary storage capacity is considered: $c_2 = 1$ (solid lines), $c_2 = 0$ (dashed lines). The remaining parameters are fixed at 1. Discretization by $\text{BDM}_1\text{-(BDM}_1\text{)}^2\text{-(P}_0\text{)}^2$ elements.

- [2] D. N. ARNOLD, R. S. FALK, AND R. WINTHER, *Multigrid in $H(\text{div})$ and $H(\text{curl})$* , *Numerische Mathematik*, 85 (2000), pp. 197–217.
- [3] F. AZNARAN, R. KIRBY, AND P. FARRELL, *Transformations for Piola-mapped elements*, arXiv preprint arXiv:2110.13224, (2021).
- [4] M. BAI, D. ELSWORTH, AND J.-C. ROEGIERS, *Multiporosity/multipermeability approach to the simulation of naturally fractured reservoirs*, *Water Resources Research*, 29 (1993), pp. 1621–1633.
- [5] G. BARENBLATT, G. ZHELTOV, AND I. KOCHINA, *Basic concepts in the theory of seepage of homogeneous liquids in fissured rocks [strata]*, *J. Appl. Math. Mech.*, 24 (1960).
- [6] N. BARNAFI, P. ZUNINO, L. DEDÈ, AND A. QUARTERONI, *Mathematical analysis and numerical approximation of a general linearized poro-hyperelastic model*, *Computers & Mathematics with Applications*, 91 (2021), pp. 202–228.
- [7] M. BIOT, *General theory of three-dimensional consolidation*, *J. Appl. Phys.*, 12 (1941), pp. 155–164.
- [8] M. BIOT, *Theory of elasticity and consolidation for a porous anisotropic solid*, *J. Appl. Phys.*, 26 (1955), pp. 182–185.
- [9] D. BOFFI, F. BREZZI, AND M. FORTIN, *Mixed finite element methods and applications*, vol. 44 of Springer Ser. Comput. Math., Springer, Heidelberg, 2013.
- [10] F. BREZZI, *On the existence, uniqueness and approximation of saddle-point problems arising from Lagrangian multipliers*, *Rev. Française Automat. Informat. Recherche Opérationnelle Sér. Rouge*, 8 (1974), pp. 129–151.

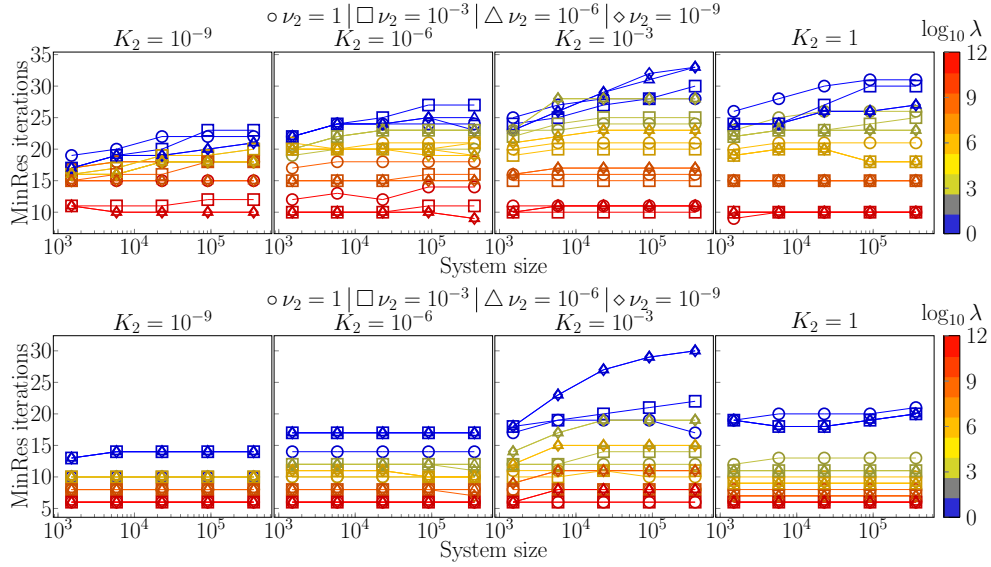


Fig. 5.7: Number of preconditioned MinRes iterations for 2-network Biot-Brinkman system with preconditioner (4.12). (Top) The displacement and flux blocks use realized by geometric multigrid while \mathcal{B}_p is computed by LU. (Bottom) Exact (LU-inverted) preconditioner is used. Transfer coefficient $\beta = 10^6$, while $c_2 = 0$, $\alpha_2 = 1$ and the remaining problem parameters are set to 1.

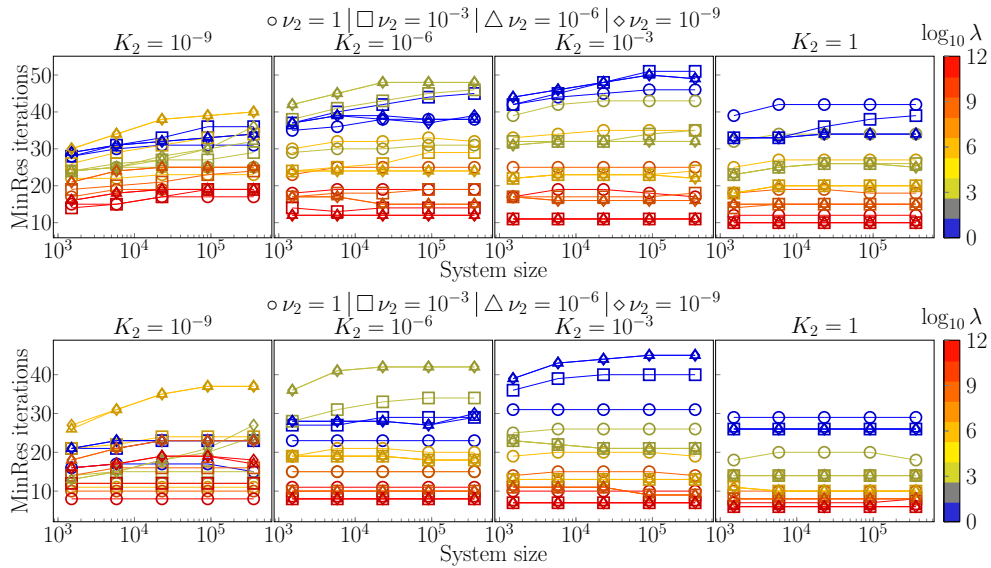


Fig. 5.8: Number of preconditioned MinRes iterations for 2-network Biot-Brinkman system with preconditioner (4.12). (Top) The displacement and flux blocks use realized by geometric multigrid while \mathcal{B}_p is computed by LU. (Bottom) Exact preconditioner is used. Transfer coefficient $\beta = 10^{-6}$, while $c_2 = 0$, $\alpha_2 = 1$ and the remaining problem parameters are set to 1.

		MinRes iterations LU				MinRes iterations MG			
		2^{-3}	2^{-4}	2^{-5}	2^{-6}	2^{-3}	2^{-4}	2^{-5}	2^{-6}
$\nu_2 \backslash h$									
	10^{-9}	43	44	45	45	46	48	50	49
	10^{-6}	43	44	45	45	46	48	50	49
	10^{-3}	39	40	40	40	45	48	51	51
	1	31	31	31	31	44	45	46	46

		Solve time LU [s]				Solve time MG [s]			
		2^{-3}	2^{-4}	2^{-5}	2^{-6}	2^{-3}	2^{-4}	2^{-5}	2^{-6}
$\nu_2 \backslash h$									
	10^{-9}	2.50	4.64	23.18	181.00	4.47	7.05	18.22	64.29
	10^{-6}	2.51	4.65	23.12	180.36	4.59	7.15	18.21	64.47
	10^{-3}	2.50	4.64	23.06	180.34	4.57	7.05	18.24	65.45
	1	2.51	4.57	22.74	178.84	4.45	6.94	17.63	62.83

Table 5.1: Performance of exact (LU) and approximate multigrid-based (MG) preconditioners for the two-network generalized Biot-Brinkman model. Parameter ν_2 is varied while $c_2 = 0$, $K_2 = 10^{-3}$, $\beta = 10^{-6}$ and the remaining parameters are set to 1. Number of unknowns in the systems ranges from 6×10^3 to 362×10^3 . Solve time aggregates setup time of the preconditioner and the run time of the Krylov solver. Computations were done in serial with threading disabled by setting `OMP_NUM_THREADS=1`.

- [11] H. C. BRINKMAN, *A calculation of the viscous force exerted by a flowing fluid on a dense swarm of particles*, Flow, Turbulence and Combustion, 1 (1949), pp. 27–34.
- [12] B. BURTSCHHELL, P. MOIREAU, AND D. CHAPELLE, *Numerical analysis for an energy-stable total discretization of a poromechanics model with inf-sup stability*, Acta Mathematicae Applicatae Sinica, 35 (2019), pp. 28–53.
- [13] R. CHABINIOK, V. Y. WANG, M. HADJICHALAMBOUS, L. ASNER, J. LEE, M. SERMESANT, E. KUHL, A. A. YOUNG, P. MOIREAU, M. P. NASH, ET AL., *Multiphysics and multiscale modelling, data-model fusion and integration of organ physiology in the clinic: ventricular cardiac mechanics*, Interface focus, 6 (2016), p. 20150083.
- [14] D. CHAPELLE AND P. MOIREAU, *General coupling of porous flows and hyperelastic formulations—from thermodynamics principles to energy balance and compatible time schemes*, European Journal of Mechanics-B/Fluids, 46 (2014), pp. 82–96.
- [15] S. CHEN, Q. HONG, J. XU, AND K. YANG, *Robust block preconditioners for poroelasticity*, Computer Methods in Applied Mechanics and Engineering, 369 (2020), p. 113229.
- [16] D. CHOU, J. VARDAKIS, L. GUO, B. TULLY, AND Y. VENTIKOS, *A fully dynamic multi-compartmental poroelastic system: Application to aqueductal stenosis*, J. Biomech., 49 (2016), pp. 2306–2312.
- [17] H. DARCY, *Les fontaines publiques de la ville de Dijon: exposition et application...*, Victor Dalmont, 1856.
- [18] E. ELISEUSSEN, M. E. ROGNES, AND T. B. THOMPSON, *A-posteriori error estimation and adaptivity for multiple-network poroelasticity*, arXiv preprint arXiv:2111.13456, (2021).
- [19] P. E. FARRELL, M. G. KNEPLEY, L. MITCHELL, AND F. WECHSUNG, *PCPATCH: Software for the topological construction of multigrid relaxation methods*, ACM Trans. Math. Softw., 47 (2021), <https://doi.org/10.1145/3445791>.
- [20] L. GUO, J. VARDAKIS, T. LASSILA, M. MITOLO, N. RAVIKUMAR, D. CHOU, M. LANGE, A. SARRAMI-FOROUSANI, B. TULLY, Z. TAYLOR, S. VARMA, A. VENNARI, A. FRANGI, AND Y. VENTIKOS, *Subject-specific multi-poroelastic model for exploring the risk factors associated with the early stages of Alzheimer’s disease*, Interface Focus, 8 (2018), p. 20170019.
- [21] P. HANSBO AND M. LARSON, *Discontinuous Galerkin and the Crouzeix-Raviart element: application to elasticity*, ESAIM: Mathematical Modelling and Numerical Analysis, 37 (2003), pp. 63–72.
- [22] Q. HONG AND J. KRAUS, *Uniformly stable discontinuous Galerkin discretization and robust iterative solution methods for the Brinkman problem*, SIAM J. Numer. Anal., 54 (2016), pp. 2750–2774.
- [23] Q. HONG AND J. KRAUS, *Parameter-robust stability of classical three-field formulation of Biot’s consolidation model*, Electron. Trans. Numer. Anal., 48 (2018), pp. 202–226.
- [24] Q. HONG, J. KRAUS, M. LYMBERY, AND F. PHILO, *Conservative discretizations and parameter-*

- robust preconditioners for Biot and multiple-network flux-based poroelasticity models*, Numerical Linear Algebra with Applications, 26 (2019), p. e2242.
- [25] Q. HONG, J. KRAUS, M. LYMBERY, AND F. PHILO, *Parameter-robust Uzawa-type iterative methods for double saddle point problems arising in Biot's consolidation and multiple-network poroelasticity models*, Mathematical Models and Methods in Applied Sciences, 30 (2020), pp. 2523–2555.
- [26] Q. HONG, J. KRAUS, M. LYMBERY, AND F. PHILO, *A new framework for the stability analysis of perturbed saddle-point problems and applications*, arXiv:2103.09357v3 [math.NA], (2021).
- [27] Q. HONG, J. KRAUS, M. LYMBERY, AND M. F. WHEELER, *Parameter-robust convergence analysis of fixed-stress split iterative method for multiple-permeability poroelasticity systems*, Multiscale Modeling & Simulation, 18 (2020), pp. 916–941.
- [28] Q. HONG, J. KRAUS, J. XU, AND L. ZIKATANOV, *A robust multigrid method for discontinuous Galerkin discretizations of Stokes and linear elasticity equations*, Numer. Math., 132 (2016), pp. 23–49.
- [29] Q. HONG, F. WANG, S. WU, AND J. XU, *A unified study of continuous and discontinuous Galerkin methods*, Science China Mathematics, 62 (2019), pp. 1–32.
- [30] J. S. HOWELL AND N. J. WALKINGTON, *Inf-sup conditions for twofold saddle point problems*, Numerische Mathematik, 118 (2011), p. 663.
- [31] R. KEDARASETTI, P. J. DREW, AND F. COSTANZO, *Arterial vasodilation drives convective fluid flow in the brain: a poroelastic model*, bioRxiv, (2021).
- [32] M. KHALED, D. BESKOS, AND E. AIFANTIS, *On the theory of consolidation with double porosity. 3. a finite-element formulation*, (1984), pp. 101–123.
- [33] J. KRAUS, P. L. LEDERER, M. LYMBERY, AND J. SCHÖBERL, *Uniformly well-posed hybridized discontinuous Galerkin/hybrid mixed discretizations for Biot's consolidation model*, Comput. Methods Appl. Mech. Engrg., 384 (2021), pp. Paper No. 113991, 23, <https://doi.org/10.1016/j.cma.2021.113991>, <https://doi.org/10.1016/j.cma.2021.113991>.
- [34] S. KUMAR, R. OYARZÚA, R. RUIZ-BAIER, AND R. SANDILYA, *Conservative discontinuous finite volume and mixed schemes for a new four-field formulation in poroelasticity*, ESAIM Math. Model. Numer. Anal., 54 (2020), pp. 273–299, <https://doi.org/10.1051/m2an/2019063>, <https://doi.org/10.1051/m2an/2019063>.
- [35] J. LEE, K.-A. MARDAL, AND R. WINTHER, *Parameter-robust discretization and preconditioning of Biot's consolidation model*, SIAM J. Sci. Comput., 39 (2017), pp. A1–A24, <https://doi.org/10.1137/15M1029473>, <http://dx.doi.org/10.1137/15M1029473>.
- [36] J. J. LEE, E. PIERSANTI, K.-A. MARDAL, AND M. E. ROGNES, *A mixed finite element method for nearly incompressible multiple-network poroelasticity*, SIAM Journal on Scientific Computing, 41 (2019), pp. A722–A747.
- [37] K.-A. MARDAL, M. E. ROGNES, AND T. B. THOMPSON, *Accurate discretization of poroelasticity without Darcy stability*, BIT Numerical Mathematics, (2021), pp. 1–36.
- [38] M. P. NASH AND P. J. HUNTER, *Computational mechanics of the heart*, Journal of elasticity and the physical science of solids, 61 (2000), pp. 113–141.
- [39] E. PIERSANTI, J. J. LEE, T. THOMPSON, K.-A. MARDAL, AND M. E. ROGNES, *Parameter robust preconditioning by congruence for multiple-network poroelasticity*, SIAM Journal on Scientific Computing, 43 (2021), pp. B984–B1007.
- [40] K. R. RAJAGOPAL, *On a hierarchy of approximate models for flows of incompressible fluids through porous solids*, Mathematical Models and Methods in Applied Sciences, 17 (2007), pp. 215–252.
- [41] F. RATHGEBER, D. A. HAM, L. MITCHELL, M. LANGE, F. LUPORINI, A. T. T. MCRAE, G.-T. BERCEA, G. R. MARKALL, AND P. H. J. KELLY, *Firedrake: Automating the finite element method by composing abstractions*, ACM Trans. Math. Softw., 43 (2016), <https://doi.org/10.1145/2998441>.
- [42] C. RODRIGO, X. HU, P. OHM, J. H. ADLER, F. J. GASPAR, AND L. ZIKATANOV, *New stabilized discretizations for poroelasticity and the Stokes' equations*, Computer Methods in Applied Mechanics and Engineering, 341 (2018), pp. 467–484.
- [43] R. SHOWALTER, *Poroelastic filtration coupled to Stokes flow*, Lecture Notes in Pure and Appl. Math., 242 (2010), pp. 229–241.
- [44] K. H. STØVERUD, M. ALNÆS, H. P. LANGTANGEN, V. HAUGHTON, AND K.-A. MARDAL, *Poroelastic modeling of Syringomyelia—a systematic study of the effects of pia mater, central canal, median fissure, white and gray matter on pressure wave propagation and fluid movement within the cervical spinal cord*, Computer methods in biomechanics and biomedical engineering, 19 (2016), pp. 686–698.
- [45] B. TULLY AND Y. VENTIKOS, *Cerebral water transport using multiple-network poroelastic theory: application to normal pressure hydrocephalus*, J. Fluid Mech., 667 (2011), pp. 188–215.

λ	$\log_2 h$					
	-3	-4	-5	-6	-7	-8
1	10	10	9	9	9	9
10^3	14	14	13	13	12	12
10^6	14	14	13	13	13	12
10^9	14	14	14	13	13	13
10^{12}	14	15	14	14	15	16

Table A.1: Number of preconditioned conjugate gradient iterations for approximating the displacement block \mathcal{B}_u of the Biot-Brinkman preconditioner. Geometric multigrid preconditioner uses $F(2, 2)$ -cycle with 3 levels and a vertex-star (damped Richardson) smoother. In all experiments $\mu = 1$.

- [46] J. VARDAKIS, D. CHOU, B. TULLY, C. HUNG, T. LEE, P. TSUI, AND Y. VENTIKOS, *Investigating cerebral oedema using poroelasticity*, Med. Eng. Phys., 38 (2016), pp. 48–57.
- [47] S. WHITAKER, *Flow in porous media I: A theoretical derivation of Darcy’s law*, Transport in porous media, 1 (1986), pp. 3–25.
- [48] R. WILSON AND E. AIFANTIS, *On the theory of consolidation with double porosity*, 20 (1982), pp. 1009–1035.

Appendix A. Components of multigrid preconditioner. In this section we report numerical experiments demonstrating robustness of geometric multigrid preconditioners for blocks \mathcal{B}_u and \mathcal{B}_v of the Biot-Brinkman preconditioner (4.12). Adapting the unit square geometry and the setup of boundary conditions from Subsection 5.3 we investigate performance of the preconditioners by considering boundedness of the (preconditioned) conjugate gradient (CG) iterations. In the following, the initial vector is set to 0 and the convergence of the CG solver is determined by reduction of the preconditioned residual norm by a factor 10^8 . Finally, both systems are discretized by BDM₁ elements.

Table A.1 confirms robustness of the $F(2, 2)$ -cycle for the displacement block of (4.12). In particular, the iterations can be seen to be bounded in mesh size and the Lamé parameter λ .

For the flux block \mathcal{B}_v we limit the investigations to the two-network case and set $c_2 = 0$, $\alpha_2 = 1$ as these parameter values yielded the stiffest problems (in terms of their condition numbers) in the robustness study of Subsection 5.2. Performance of the geometric multigrid preconditioner using a $W(2, 2)$ -cycle with vertex-star smoother is then summarized in Figure A.1. We observe that the number of CG iterations is bounded in the mesh size and variations in K_2 , ν_2 and the exchange coefficient β .

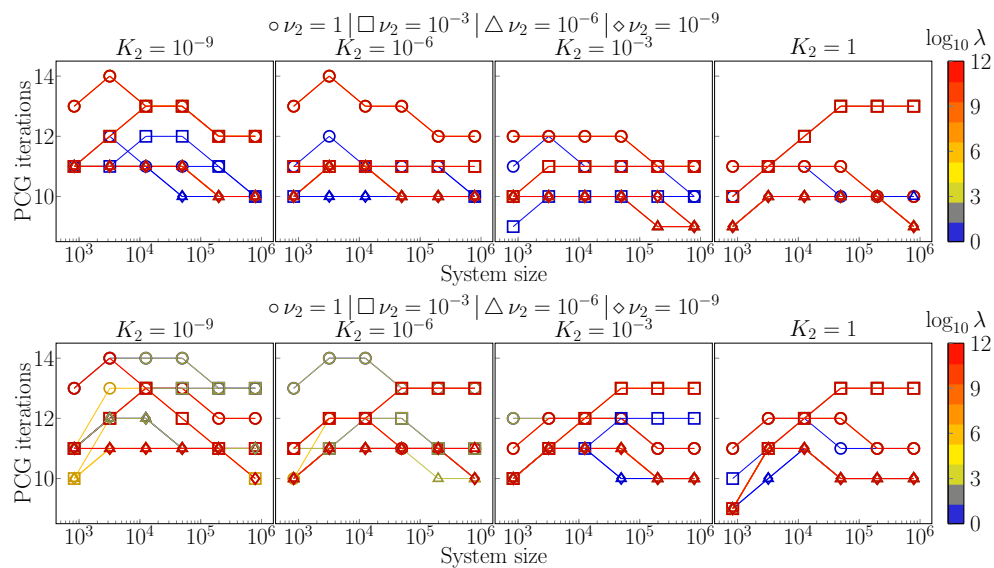


Fig. A.1: Number of preconditioned conjugate gradient iterations for approximating the flux block \mathcal{B}_v of the Biot-Brinkman preconditioner. The preconditioner uses $W(2, 2)$ -cycle of geometric multigrid with vertex-star (damped Richardson) smoother and 3 grid levels. (Top) Transfer coefficient $\beta = 10^6$, (bottom) $\beta = 10^{-6}$. Values of K_2 , ν_2 (encoded by markers) and λ (encoded by line color) are varied. In both setups $c_2 = 0$, $\alpha_2 = 1$ and the remaining problem parameters are set to 1.